MOLECULAR AND CELLULAR BIOLOGY, Oct. 2002, p. 7226–7241 Vol. 22, No. 20
0270-7306/02/$04.00+0 DOI: 10.1128/MCB.22.20.7226–7241.2002

Distinct Cell Cycle Timing Requirements for Extracellular Signal-Regulated Kinase and Phosphoinositide 3-Kinase Signaling Pathways in Somatic Cell Mitosis

Elisabeth C. Roberts,[1] Paul S. Shapiro,[2] Theresa Stines Nahreini,[3] Gilles Pages,[4] Jacques Pouyssegur,[4] and Natalie G. Ahn[3,5]*

Departments of Molecular Cellular and Developmental Biology[1] and Chemistry and Biochemistry,[3] and Howard Hughes Medical Institute,[5] University of Colorado, Boulder, Colorado 80309; Department of Pharmaceutical Sciences, University of Maryland School of Pharmacy, Baltimore, Maryland 21201[2]; and Institute of Signaling, Developmental Biology and Cancer Research, CNRS-UMR, Centre Antoine Lacassagne, 06189 Nice, France[4]

Received 20 March 2002/Returned for modification 22 April 2002/Accepted 8 July 2002

Mitogen-activated protein (MAP) kinase and phosphoinositide 3-kinase (PI3K) pathways are necessary for cell cycle progression into S phase; however the importance of these pathways after the restriction point is poorly understood. In this study, we examined the regulation and function of extracellular signal-regulated kinase (ERK) and PI3K during G_2/M in synchronized HeLa and NIH 3T3 cells. Phosphorylation and activation of both the MAP kinase kinase/ERK and PI3K/Akt pathways occur in late S and persist until the end of mitosis. Signaling was rapidly reversed by cell-permeable inhibitors, indicating that both pathways are continuously activated and rapidly cycle between active and inactive states during G_2/M. The serum-dependent behavior of PI3K/Akt versus ERK pathway activation indicates that their mechanisms of regulation differ during G_2/M. Effects of cell-permeable inhibitors and dominant-negative mutants show that both pathways are needed for mitotic progression. However, inhibiting the PI3K pathway interferes with cdc2 activation, cyclin B1 expression, and mitotic entry, whereas inhibiting the ERK pathway interferes with mitotic entry but has little effect on cdc2 activation and cyclin B1 and retards progression from metaphase to anaphase. Thus, our study provides novel evidence that ERK and PI3K pathways both promote cell cycle progression during G_2/M but have different regulatory mechanisms and function at distinct times.

Mammalian-cell proliferation requires the activation of Ras and subsequent signaling through divergent pathways involving Raf-1, mitogen-activated protein kinase kinase 1/2 (MKK1/2), and extracellular signal-regulated kinase 1/2 (ERK1/2), as well as phosphoinositide 3-kinase (PI3K), phosphoinositide-dependent kinase 1, and Akt/protein kinase B (Akt) (8, 15, 26, 34). The importance of MKK/ERK and PI3K pathways during cell cycle progression has been best defined in G_1, where activation of both pathways is needed for cyclin D1 induction, repression of cyclin kinase inhibitors, E2F activation, and entry into DNA replication. Distinct signaling mechanisms in each pathway facilitate progression through G_1/S, as well as cell growth and survival in G_1, through processes involving nuclear transcription factor phosphorylation, immediate-early gene induction, expression of cell cycle genes that direct DNA synthesis, and regulation of translational initiation.

In contrast, the importance of ERK and PI3K pathways during G_2 and mitosis has yet to be clearly defined. Although previous studies indicate that ERK promotes cdc2/cyclin B activation and M phase progression in meiotic systems such as *Xenopus laevis* oocytes (46), the role of ERK in mitotic M phase appears to vary with the experimental system. For example, some reports show that, in *Xenopus* egg extracts, depletion of ERK or inhibition of MKK has no effect on cyclic activation of cdc2/cyclin B (11, 38, 52). Other studies of *Xenopus* egg extracts and fertilized eggs show instead that elevation of ERK activity arrests cells in G_2 prior to chromosome condensation and nuclear envelope breakdown, suggesting that ERK suppresses cdc2 activation and mitotic entry (1, 7, 56). The latter involves activation of Wee1, possibly though its phosphorylation by ERK (37, 55).

For somatic cells, earlier reports reached variable conclusions concerning the timing of ERK activation during G_2/M, ranging from elevated ERK activity during G_2/M and inactivation following nocodazole treatment in CHO cells (53) to low ERK activity during S/G_2 and increased activity only after nocodazole treatment in Swiss 3T3 cells (16). Studies by our laboratory and by Zecevic et al. have demonstrated activation of MKK1/2 and ERK1/2 during mitotic onset in several mammalian cell types (48, 60). Activation and nuclear localization of active MKK and ERK occur during prophase and prior to nuclear envelope breakdown, suggesting a positive role for this pathway in early M phase. In synchronized NIH 3T3 cells, inhibiting MKK/ERK signaling using dominant-negative MKK1 or MKK1/2 inhibitor PD-98059 delayed mitotic entry by 3 or 10 h, respectively (59). This was concomitant with sustained phosphorylation of cdc2 at Tyr15, suggesting that the MKK/ERK pathway promotes M phase entry by facilitating dephosphorylation of pTyr15-cdc2 and activation of cdc2-cy-

* Corresponding author. Mailing address: Department of Chemistry and Biochemistry, University of Colorado, Boulder CO 80309. Phone: (303) 492-4799. Fax: (303) 492-2439. E-mail: natalie.ahn@colorado.edu.

clin B. In contrast, suppressing ERK by injecting mitogen-activated protein kinase phosphatase 1 (MKP1) in somatic *Xenopus* tadpole cells had no effect on cdc2 activation (57).

The role of PI3K signaling during mitosis is also somewhat contradictory in literature reports. In fertilized sea urchin eggs, inhibiting PI3K with wortmannin blocks maturation-promoting factor activation and centrosome duplication and arrests embryonic cell cycling (13). Likewise, PI3K inhibitors interfere with in vitro assays for GTP-dependent nuclear envelope assembly, consistent with a proposed role for phosphoinositide-rich membranes in envelope reformation (33). On the other hand, forkhead transcription factors in *Saccharomyces cerevisiae* form functional transcription complexes at promoter elements of yeast mitotic regulators CLB2 and SWI5 (29, 31, 44). Because active Akt phosphorylates forkhead, suppressing its nuclear translocation and subsequent transcriptional activity, PI3K signaling might be expected to interfere with mitosis by suppressing expression of mitotic cyclins. However, recent studies with NIH 3T3 cells have shown that expression of constitutively active PI3K does not affect mitotic entry but instead delays mitotic exit between M and G_1, leading to defective cytokinesis (6).

In this study, we compare the regulation and function of ERK and PI3K pathways during G_2/M in mammalian systems. Here we present the novel results that MKK/ERK and PI3K pathway components are activated prior to completion of DNA synthesis. Activation of the MKK/ERK pathway is serum dependent in NIH 3T3 cells but serum independent in HeLa cells, revealing cell-specific variations in growth factor dependence during S/G_2. Importantly, suppressing ERK activation using MKK inhibitors or dominant-negative ERK resulted in a minimal delay in cdc2 activation but delayed cyclin B1 nuclear translocation as well as progression from metaphase into anaphase. This demonstrates that ERK is important for facilitating mitotic progression after cdc2 activation and during mitotic exit, in addition to promoting mitotic entry at the level of cyclin B1 translocation. On the other hand, inhibiting PI3K signaling with a PI3K inhibitor or dominant-negative Akt arrested cells in G_2 concomitant with suppression of cyclin B1 induction and cdc2 activation. This reveals a positive role for the PI3K pathway in regulating cdc2 activation and mitotic entry, in addition to its reported negative regulation of mitotic exit. These findings reveal distinct cell cycle timing requirements for MKK/ERK versus PI3K signaling in G_2/M and provide new insight into the integration between G_1 signaling pathways and cell cycle regulation.

MATERIALS AND METHODS

Cell culture. NIH 3T3 cells, HeLa S3 cells, and ERK1$^{-/-}$ mouse embryonic fibroblasts (MEFs) were maintained in complete medium (Dulbecco's modified Eagle's medium [DMEM], 10% fetal bovine serum [FBS]) supplemented with penicillin (100 U/ml) and streptomycin (100 μg/ml). Retinal pigment epithelial cells expressing human telomerase reverse transcriptase (Clontech) were grown in DMEM–F-12 with 10% FBS, 2 mM L-glutamine, and 0.348% sodium bicarbonate. Cell synchronization was carried out by plating cells onto 6- or 10-cm-diameter dishes; cells reached 50% confluence on the following day. Cells were then treated with 2 mM thymidine in complete medium for 16 h, washed twice with Hanks' balanced saline solution (HBSS) or with DMEM–0% FBS, incubated for 8 h in complete medium, and treated again for 16 h with 2 mM thymidine in complete medium. The resulting G_1/S-enriched cells were washed twice with HBSS or DMEM–0% FBS and released into the cell cycle in the presence of DMEM–10% FBS for up to 26 h; MKK1/2 or PI3K inhibitors were added at various times. Cells switched into 0% FBS were washed three times with HBSS and then incubated in DMEM–0% FBS or OptiMEM–0% FBS. In some experiments, cells were synchronized in G_1/S and then transiently transfected with Lipofectamine (Life Technologies) during the first 3 to 4 h after release with wild-type (WT) or dominant-negative (K52R) ERK2 or WT or dominant-negative Akt1. In other experiments, cells were first transiently transfected and then synchronized and released back into the cell cycle as described above.

Reagents. Stock solutions of PD-98059 (50 mM; Calbiochem), U-0126 (10 mM; Promega), and PD-184352 (21 mM; Upstate Biotechnology) in dimethyl sulfoxide (DMSO) were diluted into media to final concentrations of 75 to 100 μM, 15 to 100 μM, and 25 μM, respectively. Stock solutions of wortmannin (400 μM; Sigma) and LY-294002 (25 mM; Sigma) were diluted into media to final concentrations of 200 nM and 25 μM, respectively. Monoclonal antibodies recognizing diphosphorylated ERK1/2 (ppERK1/2; pT183 and pY185), α-tubulin, and γ-tubulin were purchased from Sigma. Monoclonal antibodies recognizing the hemagglutinin (HA) tag epitope (12CA5) were purchased from BabCO, and monoclonal antibodies recognizing β-tubulin (3B15.9) were a gift from Dick McIntosh (39). Polyclonal antibodies recognizing phosphorylated MKK1/2 (pS217 and pS221), Akt (pS473), cdc2 (pY15), and p70 S6 kinase (pT389) were purchased from Cell Signaling Technology. Rabbit polyclonal antibodies recognizing MKK1 (C-18), Akt1/2 (H-136), ERK2 (C-14), cdc25C (C-20), and poly-(ADP-ribose) polymerase (PARP) (H-250) and monoclonal antibodies recognizing p34-cdc2 (17) and cyclin B1 (GNS1) were purchased from Santa Cruz Biotechnology. Rabbit polyclonal antibodies recognizing phosphorylated Ser10 (pH 3) of histone H3 were purchased from Upstate Biotechnology.

Cell transfections were carried out with 1 μg of plasmids for expression of rat WT or K52R ERK2 (a gift from Melanie Cobb, University of Texas Southwestern) from pMCL under the control of a cytomegalovirus (CMV) promoter and of human WT or K179M Akt from pCEFL under the control of a CMV promoter (a gift from J. Silvio Gutkind, National Institutes of Health).

Immunoblotting. Synchronized cells were washed twice with cold phosphate-buffered saline (PBS), lysed by being scraped into 300 μl of tissue lysis buffer (20 mM Tris [pH 7.4], 137 mM NaCl, 2 mM EDTA, 1% Triton X-100, 25 mM β-glycerophosphate, 2 mM sodium pyrophosphate, 10% glycerol, 1 mM sodium orthovanadate, 1 mM phenylmethylsulfonyl fluoride, 1 mM benzamidine). Lysates (20 μg) were diluted with an equal volume of 2× sodium dodecyl sulfate (SDS) sample buffer and resolved by SDS-polyacrylamide gel electrophoresis. Proteins were transferred to a polyvinylidene difluoride (PVDF) membrane, blocked for 1 to 2 h with 5% nonfat dry milk or 3% bovine serum albumin (BSA) in Tris-buffered saline (TBS; 50 mM Tris [pH 7.5], 0.15 M NaCl, 0.1% Tween 20), and incubated for 2 h to overnight with primary antibodies diluted in TBS–1% BSA. Membranes were washed several times in TBS and incubated with horseradish peroxidase-conjugated antimouse or antirabbit antibodies (Jackson ImmunoResearch; diluted 1:10,000). Proteins were detected by enhanced chemiluminescence (NEN/DuPont).

Flow cytometry. Synchronized cells were trypsinized, washed with PBS, fixed with 3 ml of cold (−20°C) 70% ethanol, and stored at 4°C overnight. Cells were then incubated with 100 μg of propidium iodide (Sigma)/ml dissolved in 0.2 M Tris, pH 7.5-20 mM EDTA–1 mg of RNase A (Sigma)/ml for 1 h at room temperature and diluted with an equal volume of PBS. DNA content was measured by flow cytometry (FACScan analyzer; Becton Dickinson) and analyzed by using the Sync Wizard model and ModFit LT software (Becton Dickinson). Aggregated cells revealed by forward scattering were filtered out of the data set prior to analysis. To quantify G_1, S, and G_2/M populations, settings for 2N and 4N peaks were defined within each experiment from the G_1/S-arrested cells and applied to all samples within a given experiment. Apoptotic cells were quantified by using the Fit Apoptosis function in the software, which determines the percentage of cells that are sub-2N, calibrated with respect to the reference G_1 peak in each experiment.

Histone H1 kinase assays. An anti-cdc2 antibody (0.4 μg) adsorbed to 10 μl of protein G-Sepharose (Pharmacia) was added to cell lysates (100 μg) and incubated with mixing at 4°C for 2 h. Immune complexes were washed extensively with cold kinase buffer (25 mM HEPES [pH 7.4], 25 mM $MgCl_2$, 1 mM dithiothreitol, 0.5 mM sodium orthovanadate) and incubated for 30 min at 30°C with 20 μl of kinase buffer containing 10 μCi of [γ-^{32}P]ATP, 20 μM cold ATP, and 2.5 μg of histone H1 (type IIIS; Sigma). Reactions were quenched with SDS loading buffer and resolved by SDS-polyacrylamide gel electrophoresis. ^{32}P incorporation into histone H1 was quantified by PhosphorImager analysis (Molecular Dynamics).

Immunofluorescence. For mitotic-index measurements, cells were grown on glass coverslips in 6-cm-diameter plates, synchronized, and transfected as described above. At various times after release, cells were fixed for 5 min with 4% paraformaldehyde in PBS (Electron Microscopy Sciences), permeabilized for 2

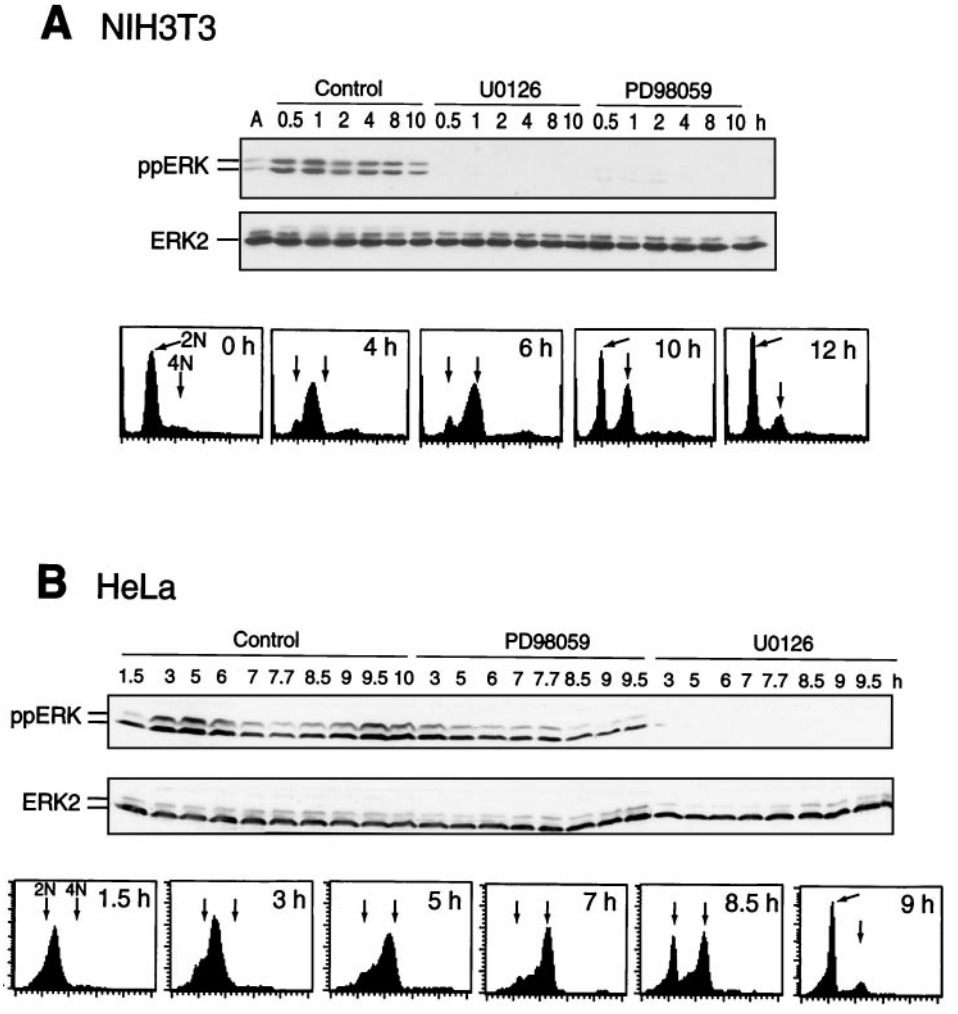

FIG. 1. Activation of ERK during S/G_2/M. Cells were synchronized by thymidine arrest, released, and harvested at the indicated times by scraping, and lysates (20 μg) were immunoblotted with an anti-ppERK or anti-ERK2 antibody. In parallel experiments, cells were analyzed by flow cytometry. (A) ERK1/2 is diphosphorylated in NIH 3T3 cells within 30 min after release and inhibited by treating cells at 0 h with 15 μM U-0126 or 75 μM PD-98059. Controls in these and other experiments were treated with an equal volume of DMSO carrier. (B) ERK1/2 is diphosphorylated in HeLa cells within 3 h after release, decreases as cells progress through G_2/M (6 to 8.5 h), and increases again as cells enter G_1. ERK phosphorylation was inhibited strongly by 25 μM U-0126 and weakly by 100 μM PD-98059.

min with 0.1% Triton X-100 in PBS, and stained for 5 min with 4′,6-diamidino-2-phenylindole (DAPI; 0.2 μg/ml in PBS). Mitotic chromosomes were identified by their characteristic condensed structures in prophase through telophase, with different fields of view at ×400 magnification analyzed. The numbers of mitotic cells were expressed as percentages of total cells counted.

For indirect immunofluorescence, cells were grown on coverslips, synchronized, and transfected and then fixed and permeabilized. Cells were immunostained with mouse anti-HA (1:1,000), mouse anti-cyclin B1 (1:500), mouse γ-tubulin (1:200), mouse α-tubulin (1:200), mouse β-tubulin (1:10), or rabbit anti-pH 3 primary antibodies (1:200), followed by goat anti-mouse AlexaFluor 488 (1:400) and goat anti-rabbit AlexaFluor 594 (1:400) secondary antibodies (Molecular Probes) with 0.2 μg of DAPI/ml as described previously (48).

RESULTS

ERK phosphorylation cycles continuously during G_2/M. HeLa or NIH 3T3 cells were synchronized in G_1/S by double-thymidine arrest and released into S phase. ERK phosphorylation was monitored at various times after release back into the cell cycle by immunoblotting with an antibody that recognizes active, diphosphorylated forms of ERK1 and ERK2. Parallel experiments monitored the cell cycle stage by flow cytometry (Fig. 1). Diphosphorylation of ERK in synchronized NIH 3T3 cells occurred within 30 min after release, peaked at 1 h, and remained sustained during G_2/M until cells returned to G_1 at 10 h (Fig. 1A). In HeLa cells, biphasic phosphorylation of ERK increased during S phase between 1.5 and 5 h after release, decreased between 6 and 8 h as cells transited G_2, and increased between 8.5 and 10 h as cells proceeded through mitosis and returned to G_1 (Fig. 1B). In both cell types, ERK phosphorylation was suppressed by MKK inhibitors U-0126 or PD-98059 (3, 5, 17), indicating that the mechanism of phosphorylation requires active MKK1/2 (Fig. 1). In HeLa cells, U-0126 was found to be a more effective inhibitor of ERK phosphorylation and activation than PD-98059 (Fig. 1B).

Incubation of HeLa cells through a second cell cycle allowed analysis of ERK phosphorylation during mitotic entry without

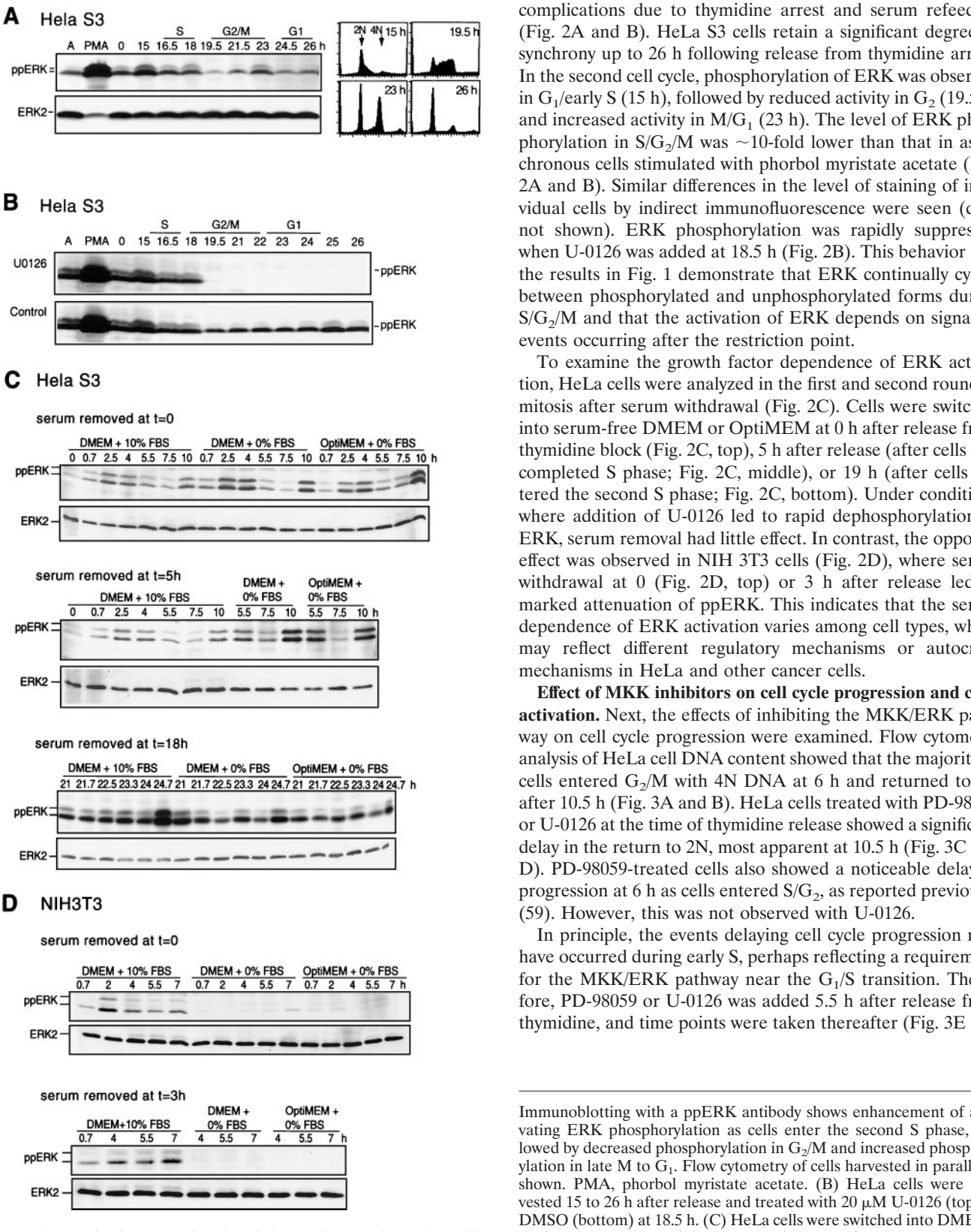

FIG. 2. Mitotic ERK phosphorylation cycles continuously. Cells were synchronized, harvested at the indicated times after release from thymidine block, and analyzed by immunoblotting with anti-ppERK or anti-ERK2. (A) HeLa cells were allowed to complete one synchronized cell cycle and then harvested 15 to 26 h after release. Immunoblotting with a ppERK antibody shows enhancement of activating ERK phosphorylation as cells enter the second S phase, followed by decreased phosphorylation in G_2/M and increased phosphorylation in late M to G_1. Flow cytometry of cells harvested in parallel is shown. PMA, phorbol myristate acetate. (B) HeLa cells were harvested 15 to 26 h after release and treated with 20 μM U-0126 (top) or DMSO (bottom) at 18.5 h. (C) HeLa cells were switched into DMEM–10% FBS, DMEM–0% FBS, or OptiMEM–0% FBS, at 0 (top), 5 (middle), or 19 h (bottom) after release. Similar results were obtained in two or three separate experiments. (D) NIH 3T3 cells were switched into DMEM–10% FBS, DMEM–0% FBS, or OptiMEM–0% FBS at 0 (top) or 3 h (bottom) after release.

complications due to thymidine arrest and serum refeeding (Fig. 2A and B). HeLa S3 cells retain a significant degree of synchrony up to 26 h following release from thymidine arrest. In the second cell cycle, phosphorylation of ERK was observed in G_1/early S (15 h), followed by reduced activity in G_2 (19.5 h) and increased activity in M/G_1 (23 h). The level of ERK phosphorylation in S/G_2/M was ~10-fold lower than that in asynchronous cells stimulated with phorbol myristate acetate (Fig. 2A and B). Similar differences in the level of staining of individual cells by indirect immunofluorescence were seen (data not shown). ERK phosphorylation was rapidly suppressed when U-0126 was added at 18.5 h (Fig. 2B). This behavior and the results in Fig. 1 demonstrate that ERK continually cycles between phosphorylated and unphosphorylated forms during S/G_2/M and that the activation of ERK depends on signaling events occurring after the restriction point.

To examine the growth factor dependence of ERK activation, HeLa cells were analyzed in the first and second round of mitosis after serum withdrawal (Fig. 2C). Cells were switched into serum-free DMEM or OptiMEM at 0 h after release from thymidine block (Fig. 2C, top), 5 h after release (after cells had completed S phase; Fig. 2C, middle), or 19 h (after cells entered the second S phase; Fig. 2C, bottom). Under conditions where addition of U-0126 led to rapid dephosphorylation of ERK, serum removal had little effect. In contrast, the opposite effect was observed in NIH 3T3 cells (Fig. 2D), where serum withdrawal at 0 (Fig. 2D, top) or 3 h after release led to marked attenuation of ppERK. This indicates that the serum dependence of ERK activation varies among cell types, which may reflect different regulatory mechanisms or autocrine mechanisms in HeLa and other cancer cells.

Effect of MKK inhibitors on cell cycle progression and cdc2 activation. Next, the effects of inhibiting the MKK/ERK pathway on cell cycle progression were examined. Flow cytometry analysis of HeLa cell DNA content showed that the majority of cells entered G_2/M with 4N DNA at 6 h and returned to G_1 after 10.5 h (Fig. 3A and B). HeLa cells treated with PD-98059 or U-0126 at the time of thymidine release showed a significant delay in the return to 2N, most apparent at 10.5 h (Fig. 3C and D). PD-98059-treated cells also showed a noticeable delay of progression at 6 h as cells entered S/G_2, as reported previously (59). However, this was not observed with U-0126.

In principle, the events delaying cell cycle progression may have occurred during early S, perhaps reflecting a requirement for the MKK/ERK pathway near the G_1/S transition. Therefore, PD-98059 or U-0126 was added 5.5 h after release from thymidine, and time points were taken thereafter (Fig. 3E and

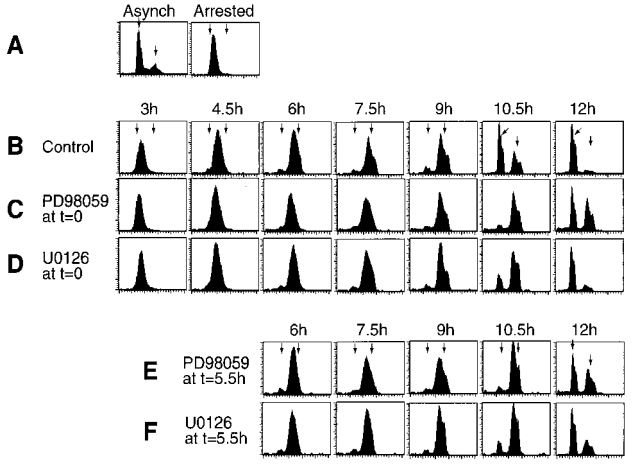

FIG. 3. Cell synchronization and effects of MKK1/2 inhibitors on S/G_2/M progression. HeLa cells were synchronized by thymidine arrest. At time zero, medium was replaced with DMEM–10% FBS and cells were analyzed at the indicated times by flow cytometry. (A) Asynchronous (Asynch) cells show peak fluorescence of 2N and 4N cells (arrows). Synchronized cells sampled before release show arrest in G_1/S. (B to D) Comparison of synchronized cells treated with DMSO (0.1% [vol/vol]) (B), PD-98059 (100 μM) (C), or U-0126 (20 μM) (D) simultaneously with release at 0 h shows a delay in progression of cells from 4N to 2N in the presence of either MKK1/2 inhibitor. (E and F) Synchronized cells treated with PD-98059 (100 μM) (E) or U-0126 (20 μM) (F) at 5.5 h after release are also delayed in progression from 4N to 2N. Similar results were obtained in three separate experiments with HeLa cells and once with NIH 3T3 cells (data not shown).

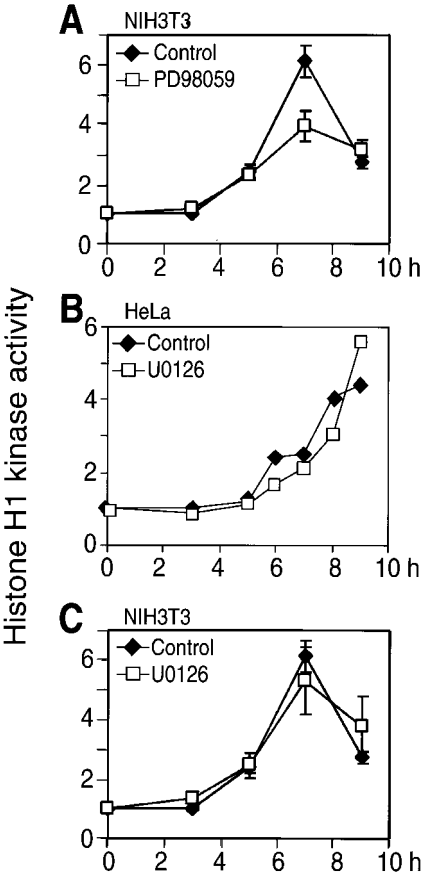

FIG. 4. Effect of MKK/ERK pathway inhibition on cdc2 activation. NIH 3T3 (A and C) and HeLa (B) cells were synchronized and released into DMSO (diamonds) or PD-98059 (100 μM) or U-0126 (20 μM) (squares). At various times, cell lysates were prepared, followed by immunoprecipitation of cdc2 and measurement of histone H1 phosphorylation, reported as fold increases normalized to time zero. Because U-0126 only slightly delayed cdc2 activation (by less than 1 h) the significant delay in kinase activation by PD-98059 was attributed to a nonspecific drug effect.

F). The effects of either inhibitor added at 5.5 h were similar to those observed when the inhibitor was added at time zero. Thus, the observed delay depends on events that require MKK/ERK pathway activation well after the restriction point and does not represent secondary effects of inhibiting the pathway during G_1.

As reported previously (59), PD-98059 also caused a significant delay in cdc2 histone H1 kinase activation in HeLa and NIH 3T3 cells (shown for NIH 3T3 cells; Fig. 4A) and delayed tyrosine dephosphorylation of cdc2 and hyperphosphorylation of cdc25C by about 90 min when added at 0 or 5.5 h (Fig. 5). However, U-0126 added at 0 h after release had little effect on cdc2 histone H1 kinase activation in either HeLa or NIH 3T3 cells (Fig. 4B and C) and little, if any, effect on cdc2 tyrosine dephosphorylation or cdc25C hyperphosphorylation when added at 0 or 5.5 h (Fig. 5). Finally, levels of cyclin B1 decreased at 12 h to ~30% of those observed at 10 h, which we attribute to degradation expected during metaphase exit. The decrease was delayed by PD-98059 but was unaffected by U-0126. Conceivably, the two compounds may act through distinct mechanisms, in which U-0126 directly suppresses MKK1/2 activity, whereas PD-98059 suppresses MKK1/2 phosphorylation and activation by upstream kinases such as Raf-1 or MEK kinase-1 (5, 17). However, neither PD-98059 nor U-0126 suppressed MKK1/2 phosphorylation after thymidine release, which was in fact augmented by both drugs to levels significantly above controls (Fig. 5A). This reflects feedback control of MKK phosphorylation (3, 5, 49). Therefore, because U-0126 is more effective than PD-98059 at inhibiting ERK phosphorylation, we conclude that inhibiting ERK has little effect on cdc2 activation and that the more pronounced effect of PD-98059 in mitosis reflects nonspecific drug behavior. Such effects render PD-98059 inappropriate for studying ERK function during G_2/M progression.

Interestingly, immunoblots of phosphorylated MKK1/2 revealed a lower-mass form of 30 kDa that was enhanced during G_2/M (Fig. 5A). This form was also observed in cells transfected with HA-MKK1 by using a probe to the N-terminal HA tag sequence (data not shown), indicating that it contains the N-terminal 30-kDa portion of MKK1. The significance of the processing product is unknown, although its appearance correlates strongly with mitotic entry, being delayed under conditions that block G_2/M progression (Fig. 5A). It may be related to previous reports of an enhanced susceptibility of MKK1 to trypsinization and production of a 20-kDa C-terminal fragment following in vitro incubation with mitotic extracts (10). In any event, limited intracellular proteolysis of MKK1/2 is a novel physiological event accompanying mitotic progression.

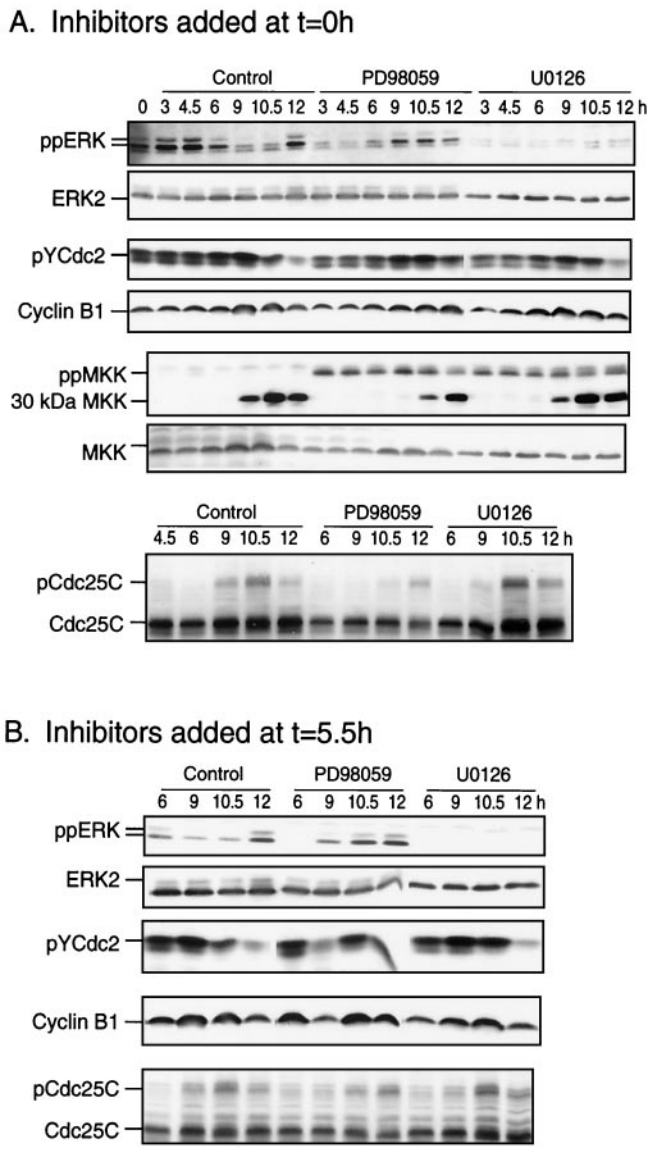

FIG. 5. Activation of ERK and MKK during S/G_2/M and effect of MKK1/2 inhibitors on mitotic cell cycle regulators. Cells were synchronized, released, and harvested at the indicated times by scraping followed by immunoblotting. (A) ERK1/2 is diphosphorylated in HeLa cells within 3 h after release, followed by decreased reactivity in G_2 and increased reactivity in late M or G_1 (12 h). ERK phosphorylation was inhibited strongly by 25 μM U-0126 and weakly by 100 μM PD-98059 added at time zero. MKK1/2 phosphorylation increased weakly after release but was elevated by addition of MKK inhibitors. The appearance of an immunoreactive species of 30 kDa, which corresponds to an N-terminal fragment of MKK, correlated with the timing of mitotic entry (9 h). Mitotic entry also correlated with decreased reactivity of pTyr15-cdc2 kinase, reflecting dephosphorylation and derepression of activity, as well as with gel mobility retardation of cdc25C phosphatase, reflecting phosphorylation and activation. U-0126 added at time zero had little effect on the behavior of cdc2, cdc25C, or the MKK fragment, although PD-98059 significantly delayed each in a manner correlating with the longer delay in recovery to 2N (Fig. 3C). No effects of MKK inhibitors on cyclin B1 were observed. (B) Addition of MKK1/2 inhibitors as for panel A except at 5.5 h after release shows similar suppression of ERK phosphorylation, indicating continuous cycling of phosphorylation in late S/G_2. Effects on cell cycle regulators are similar to those observed at time zero. Similar results were obtained in at least two separate experiments.

MKK/ERK pathway promotes early and late mitotic progression. The role of the MKK/ERK pathway in regulating mitotic progression was further characterized by monitoring chromatin staining in synchronized cells. HeLa cells synchronized in G_1/S and released back into the cell cycle in the presence of U-0126 were significantly delayed in mitotic entry compared to untreated cells (Fig. 6A). Similar results were obtained for NIH 3T3 cells with U-0126 and for HeLa cells with PD-184352, an inhibitor of MKK1/2 which is chemically unrelated to U-0126 but which most likely binds the same site on the kinase (47).

HeLa cells released from thymidine arrest were then examined for distribution among mitotic stages in the presence of increasing concentrations of U-0126 (Fig. 6B). Based on the appearance of condensed chromatin, the largest fraction of HeLa cells in prophase occurred at 7 to 8 h, with cells appearing in telophase by 9.5 h. At 7 h, the numbers of mitotic cells at all stages were reduced in the presence of U-0126, reflecting a delay in mitotic entry. However at 9.5 h, a selective decrease in anaphase and telophase cells concomitant with increased metaphase cells was also apparent, and by 10 to 10.5 h, cells treated with U-0126 were enriched in metaphase as most of the control population returned to G_1 (Fig. 6B). Representative images of cells at the 10-h time point are shown in Fig. 6C. The results demonstrate that inhibition of ERK by U-0126 suppresses the transition of cells from metaphase to anaphase and delays entry into prophase. Like U-0126, PD-184352 also interfered with mitotic entry and progression (Fig. 6D).

The delay in mitotic progression prompted us to examine the morphology of cells treated with MKK1/2 inhibitors (Fig. 6E to G). This was first examined in HeLa cells (Fig. 6E) released from thymidine arrest into 0, 25, or 100 μM U-0126 or 25 μM PD-184352. Cells analyzed at various times by indirect immunofluorescence for α- or β-tubulin, γ-tubulin, and chromatin showed no differences in spindle formation or centrosome duplication with either inhibitor. Nor were effects of the inhibitor observed in nontumorigenic NIH 3T3 and retinal pigment epithelial cell lines (Fig. 6F). Additionally, the centrosomes in NIH 3T3 cells were counted, and no apparent variation in centrosome number was observed, even at high concentrations of U-0126. These results indicated that the delayed mitotic entry and progression with U-0126 are not attributable to gross perturbations in centrosome duplication or spindle formation.

The delay in mitotic entry was further addressed in HeLa cells that were synchronized, released, and examined for subcellular localization of cyclin B1 as well as phosphorylation of histone H3 at Ser10 (pH 3), a marker of late G_2 and early M phase (4). At 7 h the majority of mitotic cells were in prophase based on chromatin appearance (Fig. 6B). At this time point, pH 3-positive cells in interphase and prophase prior to nuclear envelope breakdown were scored for weak, moderate, or strong pH 3 staining (examples in Fig. 7), which correlated, respectively with G_2, early prophase, or late prophase as determined by DAPI staining (not shown). pH 3-positive cells after prophase were not counted. We then determined the percentages of pH 3-positive cells in which cyclin B1 localization was predominantly cytoplasmic or nuclear or was equally distributed between both compartments (examples in Fig. 7). The percentages of control and U-0126-treated pH 3-positive cells with nuclear cyclin B1 were similar, with the timing of

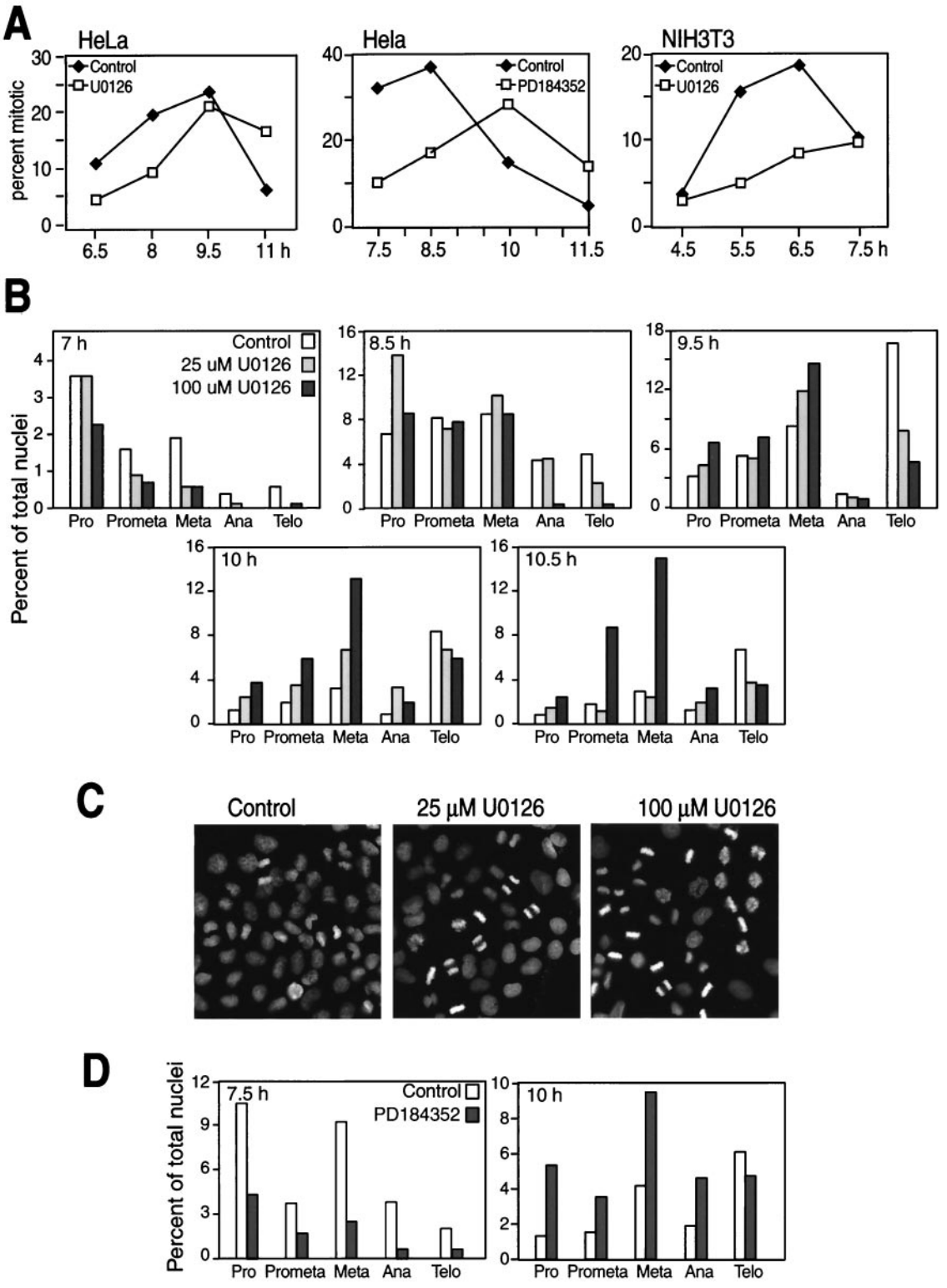

FIG. 6. MKK/ERK pathway inhibition by U-0126 delays early and late mitotic progression. (A) HeLa or NIH 3T3 cells grown on glass coverslips were synchronized and released into DMSO (diamonds) or 20 μM U-0126 or PD-184352 (squares). At various times, cells were fixed and permeabilized and chromatin was stained with DAPI. At each time point and condition, the total number of HeLa cells counted ranged between 1,100 and 2,900 and the number of NIH 3T3 cells counted ranged between 350 and 570. (B) HeLa cells grown on coverslips were synchronized, released, and treated at 5 h with 0, 25, or 100 μM U-0126. Cells were stained with DAPI at 7, 8.5, 9.5, 10, and 10.5 h and scored by chromatin appearance for numbers of cells in prophase (Pro), prometaphase (Prometa), metaphase (Meta), anaphase (Ana), and telophase (Telo). At each time point and condition, the number of HeLa cells counted ranged between 700 and 1,400, averaging 1,017 cells. (C) Cells treated with 25 or 100 μM U-0126 were monitored by DAPI staining at 10 h. At this time point, most of the control cell population returned to G_1, whereas

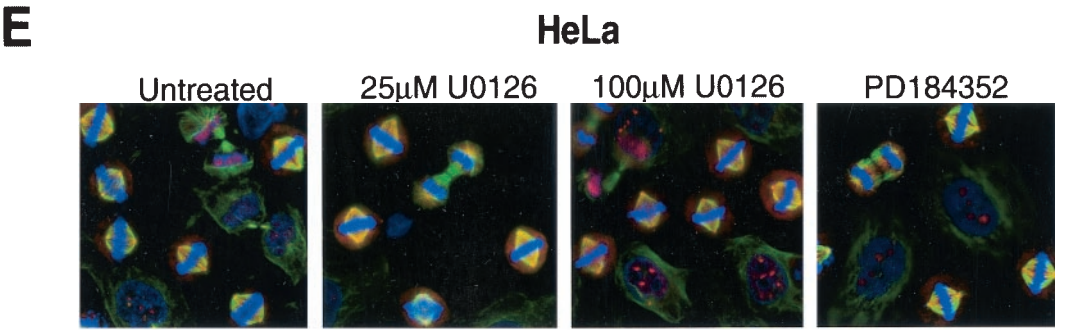

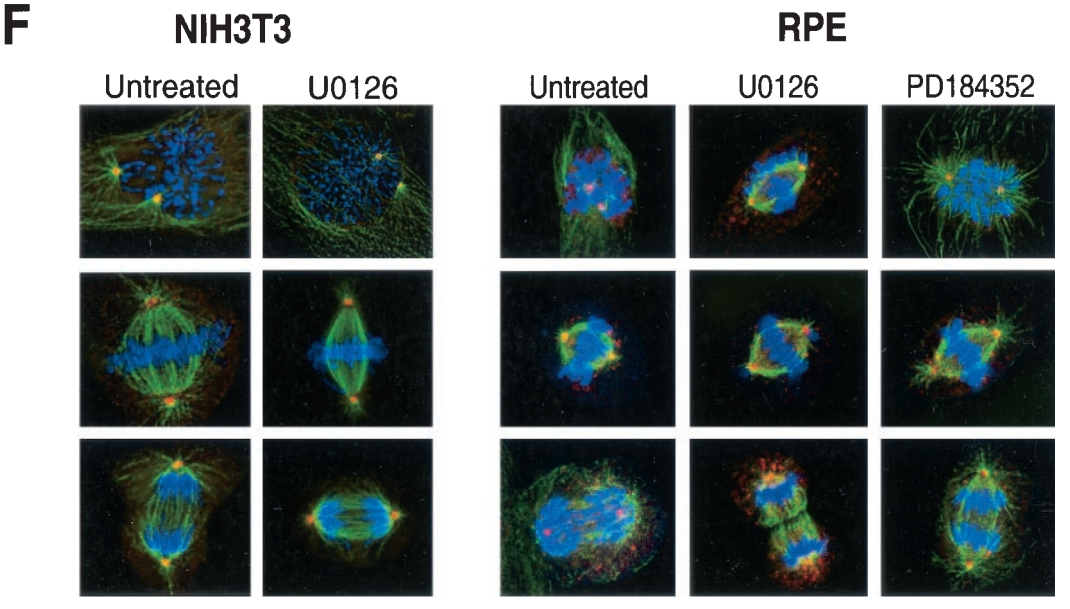

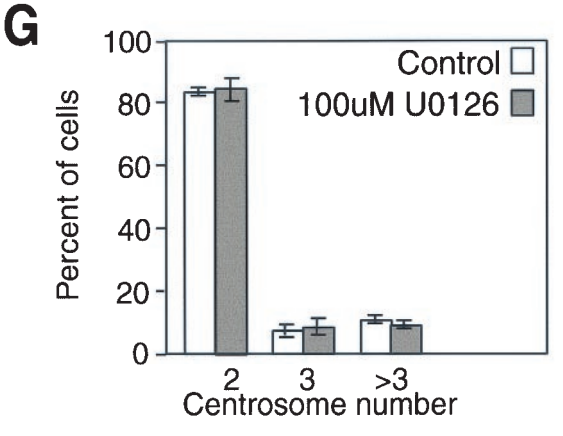

cells treated with U-0126 showed significant enrichment in metaphase. Each experiment was repeated at least twice with similar results. (D) HeLa cells grown on coverslips were synchronized, released, and treated at 5 h with 0 or 25 μM PD-184352. Cells were stained with DAPI at 7.5, 8.5, 10, and 11.5 h and scored by chromatin appearance as for panel B. At each time point and condition, the number of cells counted ranged between 1,300 and 2,900, averaging 2,100 cells. The 7.5- and 10-h time points are shown. (E) HeLa cells grown on coverslips were synchronized and released into 0, 25, or 100 μM U-0126 or 25 μM PD-184352. Cells in mitosis were analyzed by indirect immunofluorescence with anti-α-tubulin, anti-γ-tubulin, and DAPI staining. Representative images of cells at all stages of mitosis are shown. (F) NIH 3T3 cells grown on coverslips were synchronized and released into 0 or 100 μM U-0126, and retinal pigment epithelial cells (RPE) were treated with 0 or 100 μM U-0126 or 25 μM PD-184352. Mitotic cells were analyzed by indirect immunofluorescence as for panel E with anti-β-tubulin, anti-γ-tubulin, and DAPI staining. (G) Centrosomes identified by anti-γ-tubulin staining in NIH 3T3 cells as in panel F were counted at 6 and 7 h following release into 0 or 100 μM U-0126. Numbers of cells with two, three, or more than three centrosomes are indicated.

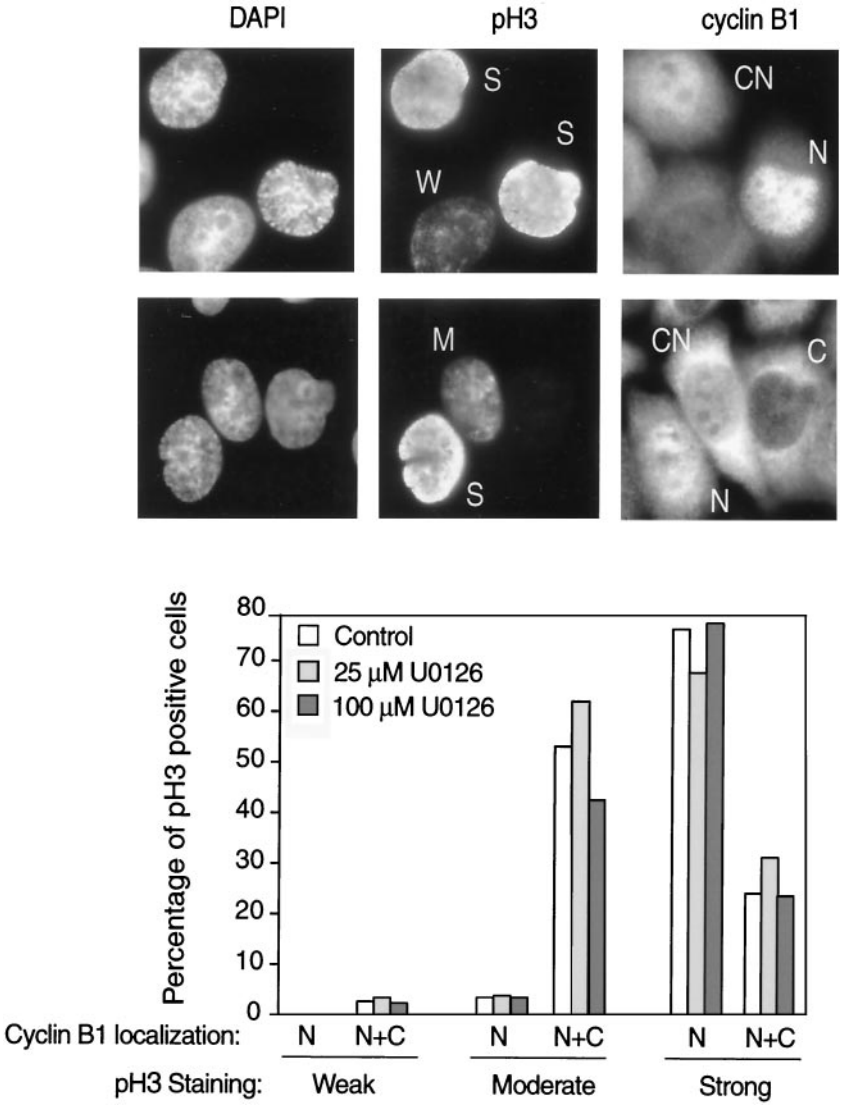

FIG. 7. Effect of U-0126 on cyclin B1 nuclear translocation. To monitor the timing of cyclin B1 nuclear translocation, cells treated with 25 or 100 μM U-0126 were analyzed at 7 h by indirect immunofluorescence with anti-cyclin B1, anti-pH 3, and DAPI staining. The pH 3-positive cells in interphase or prophase prior to nuclear envelope breakdown were counted and scored for weak, moderate, or strong pH 3 reactivity (W, M, or S, respectively, in pH 3 fluorescence images). Localization of cyclin B1 in cytoplasmic, nuclear, or both cytoplasmic and nuclear compartments (C, N, or CN, respectively, in cyclin B1 images) is reported as percentages of pH 3-positive cells, counting 100 to 150 cells in each condition.

cyclin B1 nuclear localization correlating with the degree of pH 3 staining (Fig. 7). This indicates that cyclin B1 nuclear translocation was delayed in U-0126-treated cells to the same degree as mitotic entry. Given that cyclin B1 expression levels were unaffected by U-0126 (Fig. 5), the result reveals a requirement for active ERK at or before cyclin B1 nuclear translocation.

To verify that the effects of U-0126 were due to inhibition of ERK1/2, two approaches were used to test the effects of dominant-negative ERK on the mitotic index. In the first set of experiments, HeLa cells were synchronized in G_1/S and transfected with WT or dominant-negative (K52R) ERK2 during release back into the cell cycle. Expression of recombinant ERK2 was apparent after 8 h (Fig. 8A). Under these conditions, cells were fixed onto coverslips and analyzed for mitotic index by DAPI staining. Cells expressing dominant-negative ERK2 showed a significant reduction in mitosis that was most evident in metaphase, compared to cells expressing WT ERK2 (Fig. 8B). Corresponding effects on cyclin B1 expression were minimal (Fig. 8A).

In a second approach, cell cycle progression in ERK1-deficient MEFs was examined (41). MEFs were synchronized in G_1/S with thymidine, released back into the cell cycle, and transiently transfected with HA-tagged WT or K52R ERK2 during the first 4 h after release. After release for 8 h, cells were fixed and stained to monitor recombinant ERK expression as well as pH 3 reactivity. Recombinant HA-ERK2 localized to nuclei in G_2 cells (Fig. 8C), consistent with previous reports of mitotic nuclear translocation of endogenous ERK1/2 (48, 60). Percentages of cells expressing HA-ERK2 that were also positive for pH 3 (example shown in Fig. 8C) were then calculated to monitor mitotic index. MEFs trans-

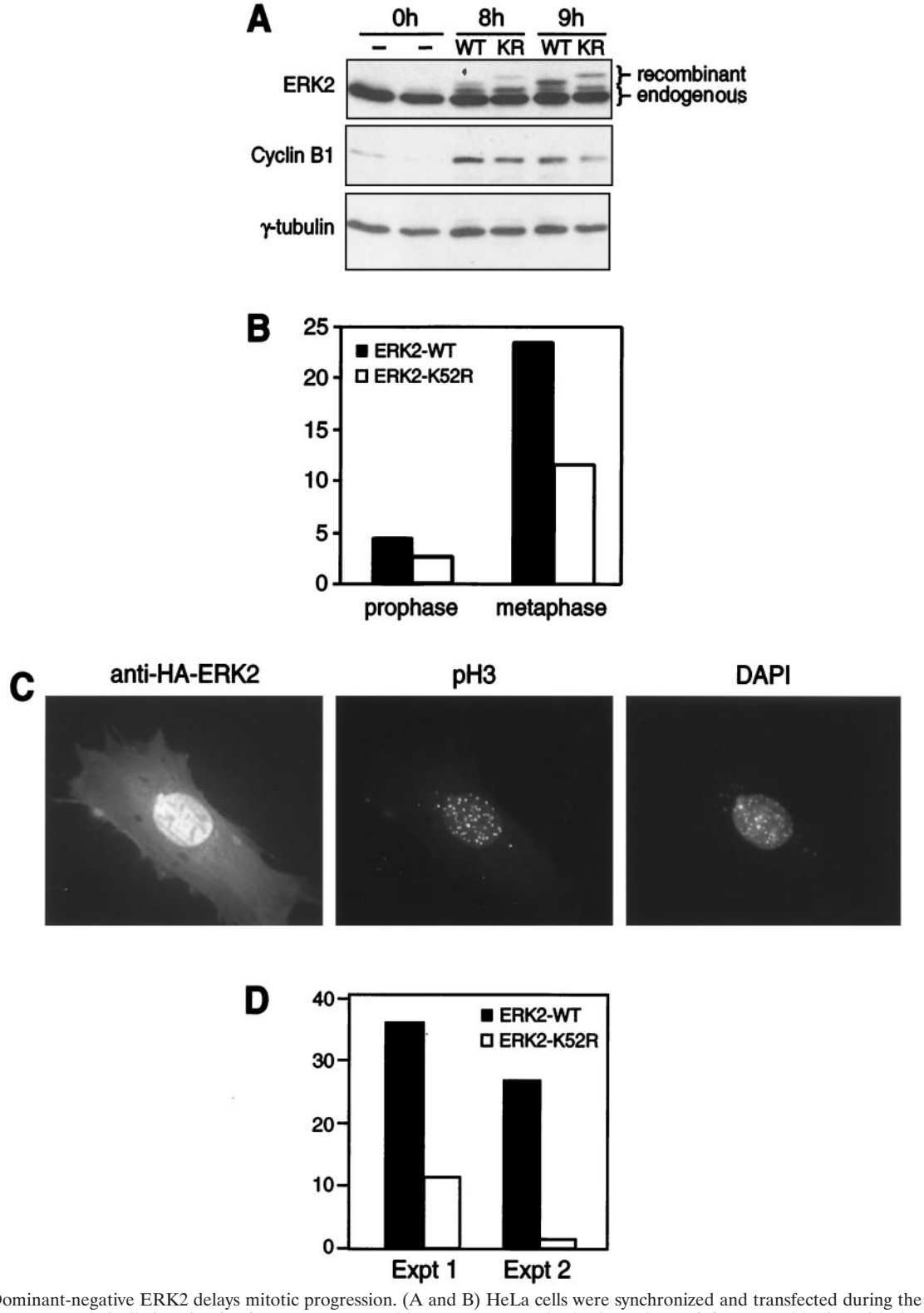

FIG. 8. Dominant-negative ERK2 delays mitotic progression. (A and B) HeLa cells were synchronized and transfected during the first 3 h of release with WT or catalytically inactive (KR) ERK2 cDNA and harvested 0, 8, and 9 h after release. (A) Immunoblotting with the anti-ERK2 antibody shows slower gel migration of recombinant WT or KR ERK2 than of endogenous ERK2 (top). Little effect of KR versus WT ERK2 on cyclin B1 levels is observed (middle). Equal protein loading is indicated by γ-tubulin immunoreactivity (bottom). (B) Cells grown and transfected in parallel on coverslips were stained 8 h after release with the anti-HA antibody and DAPI. Percentages of cells in prophase or metaphase after transfection with WT or KR ERK2 were determined based on chromatin appearance, counting 180 to 200 cells in each condition. Similar results were obtained in two independent experiments. (C) ERK1$^{-/-}$ MEFs were grown on coverslips, synchronized, and transfected during release. Cells were analyzed 8 h after release by indirect immunofluorescence, probing for recombinant HA-ERK2 (left), pH 3 reactivity (middle), and chromatin staining (right). The appearance of DAPI staining shows an example of a mitotic cell in prophase. (D) MEFs expressing WT or KR ERK2 were scored for positive reactivity with anti-pH 3 and expressed as the percentages of the total cells counted (30 to 50 cells in each condition). Two independent experiments show significant suppression of mitotic cells expressing dominant-negative ERK2.

fected with K52R ERK2 showed significantly lower pH 3 reactivity than cells transfected with WT ERK2 (Fig. 8D), corroborating the requirement for ERK signaling during progression into mitosis.

PI3K signaling promotes G_2/M progression and mitotic entry. Recent studies indicate that MKK/ERK and PI3K pathways function in early and late phases of G_1, respectively, to control entry into DNA replication (27), revealing distinct cell cycle timing requirements for each pathway during the G_1/S transition. This prompted us to examine the regulation and influence of PI3K-dependent pathways in S and G_2/M, in order to compare them to the cell cycle dependence on the MKK/ERK pathway. NIH 3T3 cells were synchronized in G_1/S and released back into the cell cycle for various times, and activation of PI3K signaling was assayed by monitoring the phosphorylation state of downstream kinases Akt and p70 S6 kinase. Enhanced phosphorylation of both Akt and p70 S6 kinase was observed within 30 min of release (Fig. 9A), similar to the kinetics of ERK activation. Phosphorylation was also enhanced during the second cell cycle following release from thymidine arrest, indicating that Akt activation during S/G_2/M is not an artifact of serum refeeding (Fig. 9B).

We next addressed the serum dependence of Akt phosphorylation (Fig. 9B and C). Significant attenuation of phosphorylated Akt was observed in HeLa cells switched into media containing 0% FBS at 0 or 18.5 h after release from thymidine block, as well as in NIH 3T3 cells switched at 0 h after release. The serum requirement of pAkt in HeLa cells contrasts with the serum independence of ppERK, indicating that the two pathways are regulated by distinct mechanisms.

To examine the requirement for signaling during cell cycle progression, PI3K inhibitors wortmannin and LY-294002 (40, 54) were added to cells at the time of release from arrest. LY-294002 effectively blocked Akt and p70 S6 kinase phosphorylation, whereas wortmannin had little effect (Fig. 9A). Likewise, LY-294002 but not wortmannin delayed S-phase exit and G_2/M entry by as much as 4 h, as measured by flow cytometry analysis of DNA content (Fig. 10A). LY-294002 also suppressed cyclin B1 expression and cdc2 histone kinase activation in NIH 3T3 cells (Fig. 9 and 10B). The effect of the PI3K inhibitor on G_2/M progression was tested in synchronized HeLa cells, where treatment with LY-294002 also suppressed cdc2 activation and cyclin B1 expression (Fig. 10C and D). Together the data reveal a novel function for PI3K in promoting cyclin B1 synthesis or stabilization and facilitating cell cycle progression at the onset of mitosis.

Enhanced apoptosis in response to LY-294002 was also observed by flow cytometry of NIH 3T3 cells synchronized and released into DMEM–10% FBS (Fig. 10E) or by PARP cleavage in HeLa cells (Fig. 10F). This indicates a second function for the PI3K pathway in promoting cell survival during mitosis, although the numbers of apoptotic cells were too low to account for the cell cycle delay.

LY-294002 inhibits other members of the PI3K gene family; therefore the effects of expressing dominant-negative Akt were examined in order to confirm the involvement of PI3K in G_2/M progression. HeLa cells were synchronized in G_1/S, transiently transfected with WT or catalytically inactive (K179M) Akt1 for 3 h, and harvested at the indicated times (Fig. 11) after release. Immunoblotting revealed a 40% reduction in cyclin B1 expression in cells transfected with inactive Akt1 compared to WT Akt1 (Fig. 11A). Under these conditions, the transient-transfection efficiency was 30%, suggesting that cyclin B1 is strongly reduced in cells expressing dominant-negative Akt. Similarly, cells that were first transfected with inactive Akt1, followed by cell synchronization and release, showed significant inhibition of cyclin B1 expression during G_2/M compared to cells transfected in parallel with WT Akt1 (Fig. 11B). The results support a novel role for both PI3K and Akt in promoting G_2/M progression at the level of cyclin B1.

Finally, the potential influence of PI3K inhibitors on ERK activation during S/G_2/M was examined to screen for potential interrelationships between the pathways. Neither LY-294002 nor wortmannin significantly affected the phosphorylation of ERK1/2 or MKK1/2 (Fig. 9A), indicating that ERK activation is not controlled by PI3K signaling. However, LY-294002 blocked proteolytic processing of MKK1/2, which correlates strongly with mitotic entry (Fig. 9A), consistent with the corresponding delay in cdc2 activation. Similarly, inhibition of MKK1/2 by U-0126 had no effect on the phosphorylation of Akt or p70 S6 kinase in synchronized cells (data not shown). Thus, ERK and PI3K pathways are both activated during G_2/M but function independently, with temporal requirements before the onset of mitosis and an additional requirement for ERK during metaphase-anaphase progression.

DISCUSSION

This study provides novel insight into the regulation and function of ERK and PI3K signaling pathways during S/G_2/M in somatic mammalian cells. Whereas previous reports showed that ERK is active during prophase (48, 60), we now demonstrate that the initial activation of both ERK and PI3K occurs in S phase. The rapid responses to cell-permeable inhibitors indicate that each pathway is continuously activated through the end of mitosis. Thus both pathways, which play critical roles during G_1, also function well after the restriction point in somatic cells.

The serum dependence of ERK activation in NIH 3T3 cells suggests that the mechanism(s) regulating this pathway is normally growth factor regulated, whereas serum independence in HeLa cells could reflect autocrine or cell-autonomous mecha-

FIG. 9. Enhancement of PI3K signaling during S/G_2/M and suppression by a PI3K inhibitor. (A) NIH 3T3 cells were synchronized and released into DMEM–10% FBS in the presence of DMSO (0.1% [vol/vol]), wortmannin (200 nM), or LY-294002 (25 μM) added at 0 h. Cells were harvested at the indicated times, and clarified lysates were analyzed by immunoblotting for activating phosphorylation of Akt, p70 S6 kinase, ERK, and MKK. Decreased signaling to Akt and p70 S6 kinase was observed in cells treated with LY-294002 in a manner that correlated with decreased cyclin B1 protein. Loading controls are shown by γ-tubulin staining. Similar results were obtained in two or three separate experiments. (B) HeLa cells were switched into DMEM–10% FBS or DMEM–0% FBS at 0 (top) or 18.5 h (bottom) after release, harvested at the indicated times, and analyzed by immunoblotting for pS473-Akt and Akt. (C) NIH 3T3 cells were switched into DMEM–10% FBS or DMEM–0% FBS at 0 h after release, harvested, and analyzed by immunoblotting as in panel B.

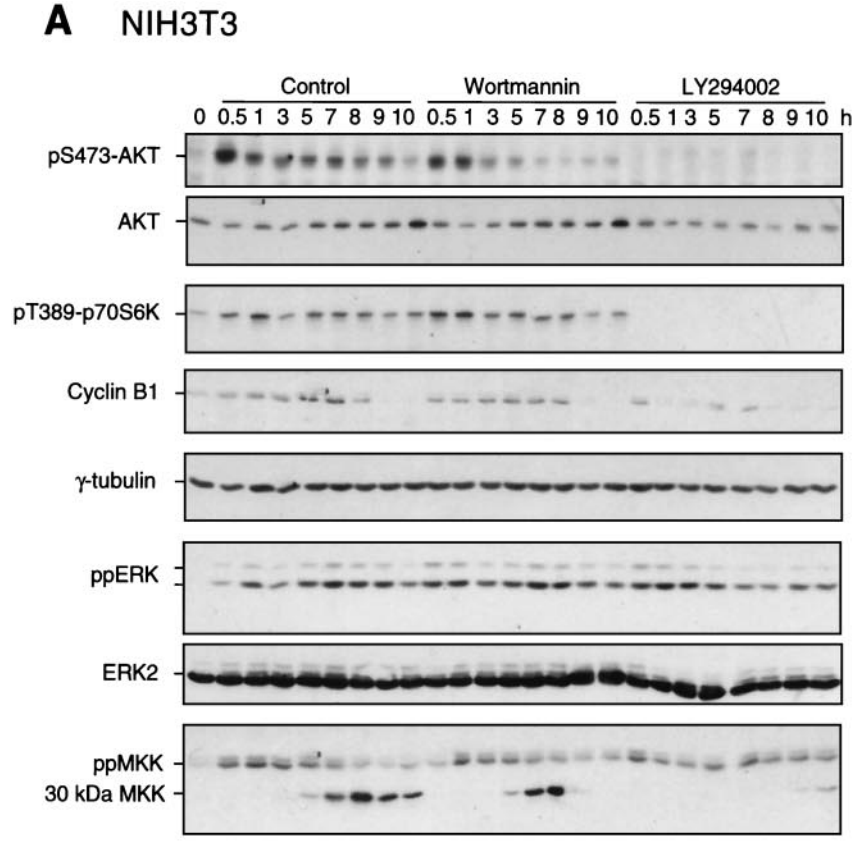
A
NIH3T3
Control
Wortmannin
LY294002
0 0.5 1 3 5 7 8 9 10 0.5 1 3 5 7 8 9 10 0.5 1 3 5 7 8 9 10 h
pS473-AKT
AKT
pT389-p70S6K
Cyclin B1
γ-tubulin
ppERK
ERK2
ppMKK
30 kDa MKK

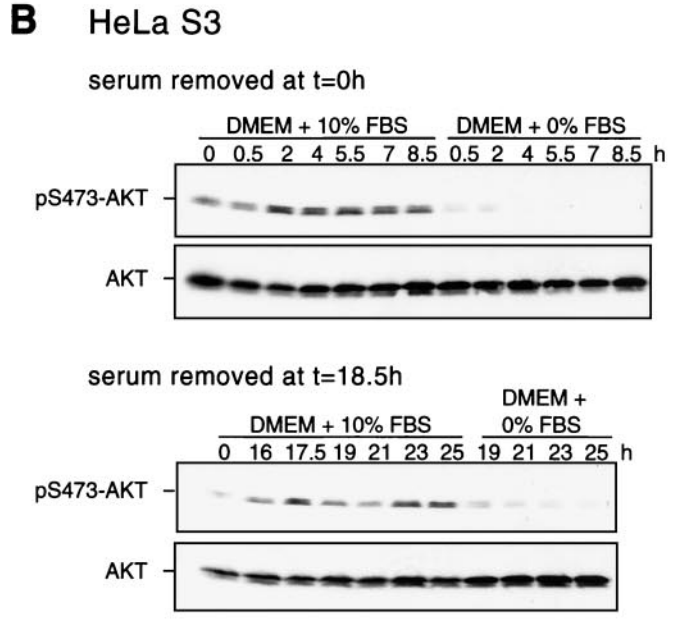
B
HeLa S3
serum removed at t=0h
DMEM + 10% FBS
DMEM + 0% FBS
0 0.5 2 4 5.5 7 8.5 0.5 2 4 5.5 7 8.5 h
pS473-AKT
AKT
serum removed at t=18.5h
DMEM + 10% FBS
DMEM + 0% FBS
0 16 17.5 19 21 23 25 19 21 23 25 h
pS473-AKT
AKT

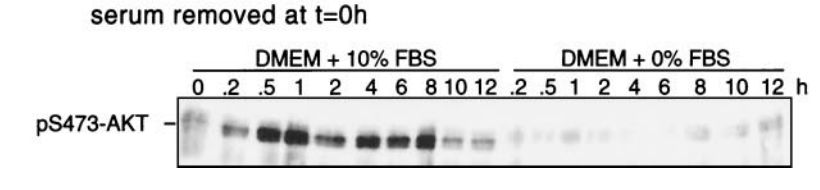
C
NIH3T3
serum removed at t=0h
DMEM + 10% FBS
DMEM + 0% FBS
0 .2 .5 1 2 4 6 8 10 12 .2 .5 1 2 4 6 8 10 12 h
pS473-AKT

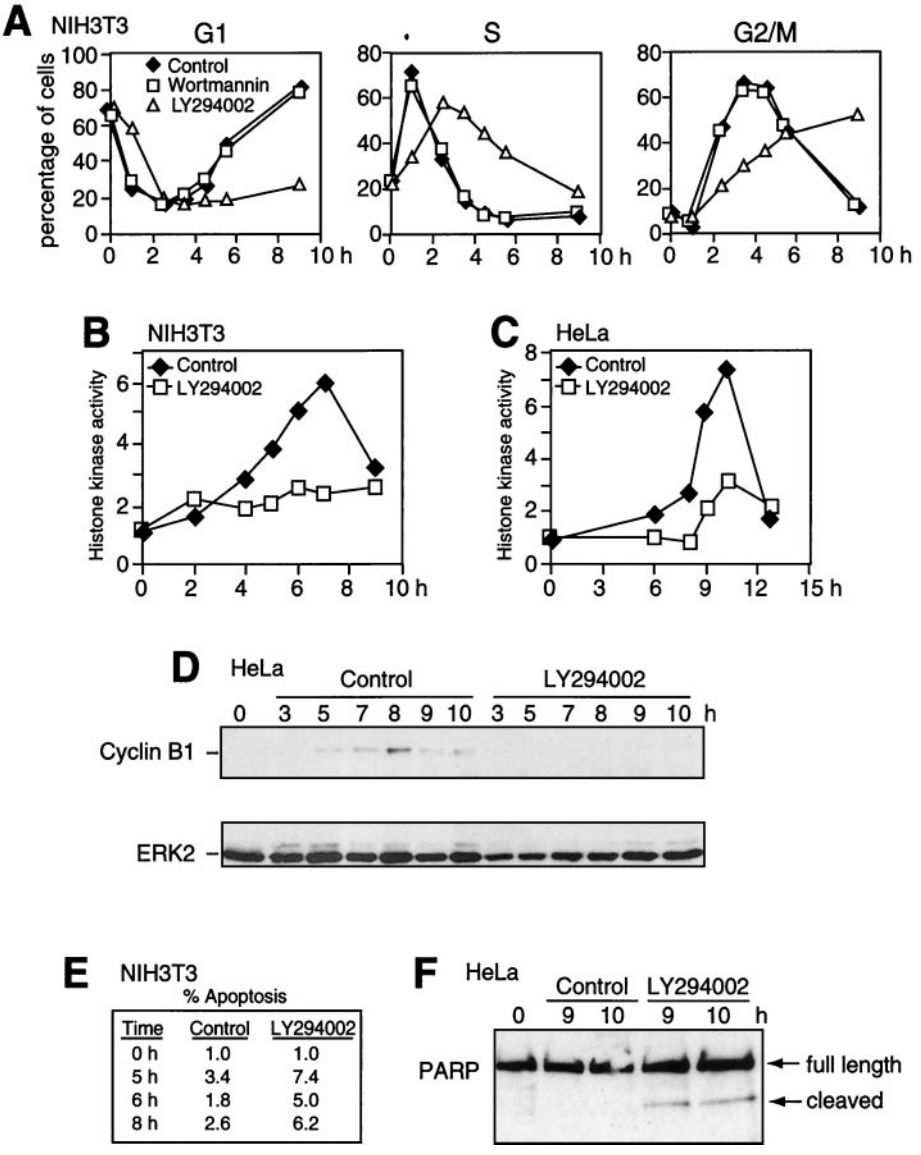

Time	Control	LY294002
0 h	1.0	1.0
5 h	3.4	7.4
6 h	1.8	5.0
8 h	2.6	6.2

FIG. 10. Inhibition of PI3K suppresses cdc2 activation and cyclin B1 induction. NIH 3T3 (A, B, and E) and HeLa (C, D, and F) cells were synchronized and released into DMEM–10% FBS in the presence of DMSO (0.1% [vol/vol]), wortmannin (200 nM), or LY-294002 (25 μM) added at 0 h. (A) NIH 3T3 cells were harvested at the indicated times, followed by flow cytometry after release into DMSO (diamonds), wortmannin (squares), or LY-294002 (triangles). Cells in G_1 (2N), S, and G_2/M (4N) were quantified by curve-fitting FACScan profiles and reported as percentages of total cells. LY-294002 caused a significant delay in S phase exit and G_2/M entry, correlating with inhibition of PI3K signaling. (B and C) NIH 3T3 (B) and HeLa (C) cells were harvested after release into DMSO (diamonds) or LY-294002 (squares). Histone H1 kinase activity measured following cdc2 immunoprecipitation from lysates show suppression of kinase activation by LY-294002. (D) HeLa cells were synchronized and released into DMSO or LY-294002, and lysates were analyzed by immunoblotting. LY-294002 causes a significant reduction in cyclin B1 expression, as observed in NIH 3T3 cells (Fig. 8). (E) NIH 3T3 cells released into DMSO or LY-294002 and analyzed by flow cytometry show increased apoptotic-cell populations (fluorescence intensity less than 2N) in the presence of a PI3K inhibitor. (F) HeLa cells synchronized and released into LY-294002 also show enhanced cleavage of PARP.

nisms. Potential upstream effectors of MKK and ERK include Src family tyrosine kinases and protein tyrosine phosphatase-α, which reportedly function in mitotic Raf activation (32, 43, 45, 61, 62). In addition, Ras signaling in G_2, which has been proposed to facilitate cyclin D1 induction (22, 23), may also be relevant to MKK/ERK pathway activation and function during G_2/M.

When ERK phosphorylation or PI3K signaling was inhibited with cell-permeable inhibitors, synchronized cells responded by delayed cell cycle progression, effects that were corroborated by expressing dominant-negative ERK and Akt mutants, respectively. However, whereas inhibition of the MKK/ERK pathway delayed mitotic entry and progression in late mitosis with little effect on cyclin B1 expression or cdc2 activation, inhibition of the PI3K/Akt pathway blocked mitotic onset, suppressing cyclin B1 induction and cdc2 activation. The findings demonstrate that somatic mammalian cells have very distinct temporal requirements for signal transduction pathways in mi-

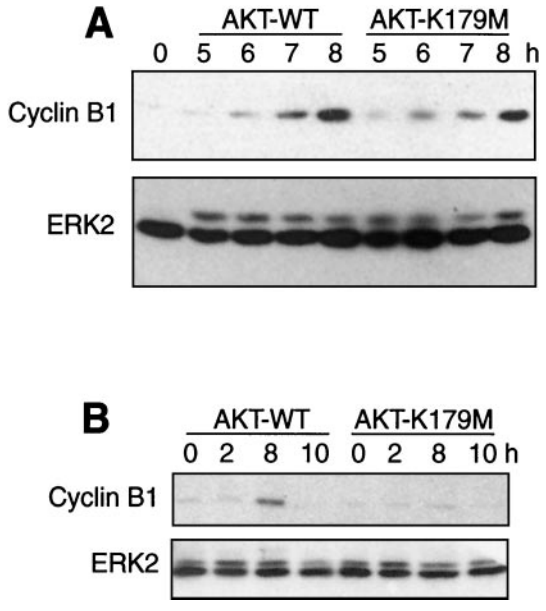

FIG. 11. Dominant-negative Akt1 suppresses cyclin B1 expression. (A) HeLa cells were synchronized and transfected during the first 3 h of release with WT or catalytically inactive (K179M) Akt and harvested 5 to 8 h after release. Immunoblotting with the cyclin B1 antibody shows reduced expression in cells expressing the Akt K179M mutant compared to that in cells expressing WT Akt (top). The transfection efficiency under these conditions was approximately 30%. Equal protein loading is indicated by ERK2 immunoreactivity (bottom). (B) The Akt K179M mutant also suppresses cyclin B1 expression when HeLa cells are first transfected with Akt for 16 h, followed by cell synchronization by double-thymidine arrest and release for 2 to 10 h.

tosis, utilizing PI3K signaling to facilitate M phase entry and MKK/ERK signaling to facilitate M phase exit to G_1.

Our initial expectation was that inhibiting the MKK/ERK pathway would substantially retard mitotic entry based on responses in *Xenopus* meiotic M phase showing inhibition of progesterone- or Mos-induced maturation and cdc2 activation following injection of neutralizing anti-MKK1 antibodies, dominant-negative MKK1, MKP1, or PD-98059 (11, 24, 30). Similarly, a report concerning NIH 3T3 cells showed a substantial delay in cdc2 activation after treatment with PD-98059 and a smaller but significant delay after expressing dominant-negative MKK1 (59). However, recent findings have raised questions about the requirement for ERK signaling in meiotic M phase. In *Xenopus* oocytes, inhibition of MKK1/2 by U-0126 does not affect progesterone-induced cdc2 and cyclin B activation or meiosis I, whereas dominant-negative *Xenopus* polo kinase (Plx1) inhibits both events (20). Thus, the MKK/ERK pathway appears to be sufficient but not necessary for entry into meiosis I, when Plx1 is active toward cdc25. Likewise, the pronounced effect of PD-98059 on mitotic entry is likely nonspecific. Taken together, we conclude that the MKK/ERK pathway is not necessary for cdc2 activation during somatic-cell mitosis, although it facilitates mitotic entry at the level of cyclin B1 nuclear translocation. It will be informative to examine the effects of U-0126 on phosphorylation events that regulate cyclin B1 import and export.

Candidate mitotic targets for ERK include the hSWI/SNF chromatin-remodeling complex, which is phosphorylated and inactivated by ERK (51), and Myt1, a cdc2-inhibitory tyrosine kinase which is phosphorylated and inactivated by pp90-Rsk (42). A role for MKK1 in Golgi dispersion during mitosis has also been suggested (2, 10, 25, 28). Earlier studies also reported that ERK depolymerizes interphase microtubules and forms mitotic microtubules in *Xenopus* cell extracts (19). In three cell lines tested, suppressing ERK with U-0126 does not noticeably perturb early mitotic events such as centrosome duplication and mitotic spindle assembly (Fig. 6E to G). These preliminary findings do not exclude regulatory mechanisms in early G_2/M but suggest that the requirements, if any, are subtle.

In *Xenopus* cycling egg extracts, ERK activation promotes spindle checkpoint arrest (36, 52), observed in the presence of nocodazole and high levels of sperm nuclei. Inhibiting ERK by adding MKP1 or PD-98059 or by immunodepleting MKK or ERK interrupts the checkpoint mechanism, causing degradation of cyclin B, release from arrest, and premature exit from mitosis, while adding Mos, MKK, or ERK to extracts sustains the mitotic state even in conditions under which cdc2 is inactivated (9, 11, 21, 36, 52). Furthermore, active ERK localizes to kinetochores in mammalian cells and its activity is stabilized by nocodazole and reduced upon anaphase entry (48, 60). We have found that potential substrates for ERK are kinetochore antigens recognized by the 3F3/2 monoclonal antibody, whose phosphorylation state is linked to microtubule attachment and tension at kinetochores (12, 48). Another potential substrate is the centromeric motor protein, CENP-E, which is involved in chromosome congression and which is directly phosphorylated by ERK (58, 60). Thus, ERK may function to provide an early sensory signal for improper microtubule-kinetochore attachment, which sustains spindle checkpoint activation.

It was therefore unexpected to observe enrichment of metaphase cells in response to U-0126, revealing that, in HeLa cells, the MKK/ERK pathway facilitates exit from metaphase. This appears to contradict a role for this pathway in promoting checkpoint activation but may be explained by the observation that, although U-0126 in our experiments eliminates most of the phosphorylated ERK in mitotic cells, it does not reduce the small pool of phosphorylated ERK associated with kinetochores (P. Shapiro, E. Roberts, and N. Ahn, unpublished data). This indicates that the soluble pool of active ERK turns over more rapidly than the kinetochore-bound pool and suggests that multiple events are controlled by the MKK/ERK pathway in late mitosis. We speculate that mitotic functions vary depending on kinase localization; for example, kinetochore-bound ppERK may be stably phosphorylated and may promote spindle checkpoint activation until microtubule attachment, whereas cytoplasmic ppERK may rapidly cycle between phosphorylated and unphosphorylated forms and promote events that facilitate exit from mitosis.

The observed suppression of cdc2 activation by PI3K inhibitors and dominant-negative Akt could be accounted for by the block in cyclin B1 protein induction. This was also unexpected, given evidence for yeast that cyclin B transcription is enhanced by forkhead, which in mammalian systems is under negative control by PI3K. However, alternative mechanisms for regulating cyclin B stability by PI3K may exist. In HeLa and other mammalian cells, PI3K transcriptionally represses CDK inhibitor p27 via phosphorylation and nuclear exclusion of forkhead

transcription factors; consequently, PI3K inhibitors such as LY-294002 induce expression of p27 (14, 18). Previous studies have also shown that inactivation of E2F or cdk2-cyclin A in mid-S phase elevates cyclin B1 ubiquitination and degradation by derepressing the association between the anaphase-promoting complex (APC) and its substrate recognition subunit, Cdh1 (35), implying that cyclin A and cdk2 activation in mid-S phase is needed for buildup of the cyclin B1 protein in G_2. Our findings may be explained by a model in which inhibition of PI3K by LY-294002 or dominant-negative Akt enhances p27 synthesis and inactivates cyclin A and cdk2, leading to destabilization of the cyclin B1 protein. While our manuscript was under review, Shtivelman et al. (50) reported results similar to ours with respect to PI3K/Akt pathway activation during G_2/M and suppression of mitotic progression by LY-294002 and also found that LY294002 causes Chk1 activation in the absence of DNA damage. Together, our two studies indicate that PI3K/Akt signaling is needed at two points during S/G_2/M, during induction of cyclin B1 and repression of Chk1.

It is instructive to compare our results with a recent report showing that expression of constitutively active PI3K (p110-CAAX) in NIH 3T3 cells increases the proportion of cells in telophase and impairs cytokinesis following release from Colcemid but has little effect on mitotic entry (6). The effect involves repression of forkhead, because the cytokinesis defect is bypassed by an Akt-insensitive FKHRL1 mutant, and transcriptionally inactive forkhead mutant ΔDBAFX mimics the effect of p110-CAAX. Although forkhead promotes transcription of mitotic cyclins in mammalian cells as it does in yeast, the repression of cyclin B transcription by p110-CAAX is not sufficient to completely downregulate cyclin B protein in G_2. This is consistent with the phenotype of *S. cerevisiae* fkh2Δ and fkh1Δfkh2Δ mutant strains, which show defects in spindle formation and cell separation but which do not arrest in G_2 (44). The mechanism for the cytokinesis defect is instead attributed to interference with cyclin B degradation during Colcemid release, possibly due to downregulation of Plk1, another transcriptional target of forkhead, which facilitates APC-mediated ubiquitination of cyclin B. Thus, mechanisms for transcriptional regulation of cyclin B by PI3K may not be as important as mechanisms for regulating protein stability after the restriction point.

Taken together, results from this study indicate that PI3K signaling, like MKK/ERK signaling, both positively and negatively affects mitotic progression. On one hand, suppressing PI3K signaling with LY-294002 or dominant-negative Akt represses mitotic entry. On the other hand, constitutive PI3K signaling disrupts cytokinesis by repressing forkhead and downregulating cyclin B and Plk1, but not enough to block mitotic entry (6). Both the loss of cyclin B1 expression by inhibiting PI3K before entry into mitosis and the loss of cyclin B1 degradation by activating PI3K during mitotic exit are consistent with a mitotic role for PI3K in suppressing APC activity. We speculate that the timing and/or localization of PI3K signaling during G_2 may be critical for regulating distinct mitotic events. Alternatively, signal transduction thresholds may be important, in which PI3K signaling must remain below a high threshold to enable transcription of mitotic regulators but must remain above a lower threshold to repress p27 and enable mitotic entry.

ACKNOWLEDGMENTS

We are indebted to Tin Tin Su, Mark Winey, and Dick McIntosh for antibodies and insightful discussions and to Melanie Cobb and J. Silvio Gutkind for gifts of ERK and Akt expression plasmids. Thanks also to Natalie Wehman, U. Maryland Cancer Center, and Xuedong Liu and Mark Winey, U. Colorado, for generous assistance with flow cytometry and microscopy.

This study was supported by grants from the Searle Scholars Program (N.G.A.) and the Concern Foundation (P.S.S.) and by NIH grants RO1 GM48521 (N.G.A.) and F32 GM18151 (P.S.S.).

E. C. Roberts and P. S. Shapiro contributed equally to this work.

REFERENCES

1. **Abrieu, A., D. Fisher, M. N. Simon, M. Doree, and A. Picard.** 1997. MAPK inactivation is required for the G_2 to M-phase transition of the first mitotic cell cycle. EMBO J. **16:**6407–6413.
2. **Acharya, U., A. Mallabiabarrena, J. K. Acharya, and V. Malhotra.** 1998. Signaling via mitogen-activated protein kinase kinase (MEK1) is required for Golgi fragmentation during mitosis. Cell **92:**183–192.
3. **Ahn, N. G., T. S. Nahreini, N. S. Tolwinski, and K. A. Resing.** 2001. Pharmacologic inhibitors of MKK1 and MKK2. Methods Enzymol. **332:**417–431.
4. **Ajiro, K., and T. Nishimoto.** 1985. Specific site of histone H3 phosphorylation related to the maintenance of premature chromosome condensation. Evidence for catalytically induced interchange of the subunits. J. Biol. Chem. **260:**15379–15381.
5. **Alessi, D. R., A. Cuenda, P. Cohen, D. T. Dudley, and A. R. Saltiel.** 1995. PD 098059 is a specific inhibitor of the activation of mitogen-activated protein kinase kinase in vitro and in vivo. J. Biol. Chem. **270:**27489–27494.
6. **Alvarez, B., A. C. Martinez, B. M. Burgering, and A. C. Carrera.** 2001. Forkhead transcription factors contribute to execution of the mitotic programme in mammals. Nature **413:**744–747.
7. **Bitangcol, J. C., A. S. Chau, E. Stadnick, M. J. Lohka, B. Dicken, and E. K. Shibuya.** 1998. Activation of the p42 mitogen-activated protein kinase pathway inhibits Cdc2 activation and entry into M-phase in cycling *Xenopus* egg extracts. Mol. Biol Cell **9:**451–467.
8. **Blume-Jensen, P., and T. Hunter.** 2001. Oncogenic kinase signalling. Nature **411:**355–365.
9. **Chau, A. S., and E. K. Shibuya.** 1998. Mos-induced p42 mitogen-activated protein kinase activation stabilizes M-phase in *Xenopus* egg extracts after cyclin destruction. Mol. Biol Cell. **9:**565–572.
10. **Colanzi, A., T. J. Deerinck, M. H. Ellisman, and V. Malhotra.** 2000. A specific activation of the mitogen-activated protein kinase kinase 1 (MEK1) is required for Golgi fragmentation during mitosis. J. Cell Biol. **149:**331–339.
11. **Cross, D. A., and C. Smythe.** 1998. PD 98059 prevents establishment of the spindle assembly checkpoint and inhibits the G_2-M transition in meiotic but not mitotic cell cycles in *Xenopus*. Exp. Cell Res. **241:**12–22.
12. **Daum, J. R., S. Tugendreich, L. M. Topper, P. M. Jorgensen, C. Hoog, P. Hieter, and G. J. Gorbsky.** 2000. The 3F3/2 anti-phosphoepitope antibody binds the mitotically phosphorylated anaphase-promoting complex/cyclosome. Curr Biol. **10:**R850–R852.
13. **De Nadai, C., P. Huitorel, S. Chiri, and B. Ciapa.** 1998. Effect of wortmannin, an inhibitor of phosphatidylinositol 3-kinase, on the first mitotic divisions of the fertilized sea urchin egg. J. Cell Sci. **111:**2507–2518.
14. **Dijkers, P. F., R. H. Medema, C. Pals, L. Banerji, N. S. Thomas, E. W. Lam, B. M. Burgering, J. A. Raaijmakers, J. W. Lammers, L. Koenderman, and P. J. Coffer.** 2000. Forkhead transcription factor FKHR-L1 modulates cytokine-dependent transcriptional regulation of p27(KIP1). Mol. Cell. Biol. **20:**9138–9148.
15. **Downward, J.** 2001. The ins and outs of signalling. Nature **411:**759–762.
16. **Edelmann, H. M., C. Kuhne, C. Petritsch, and L. M. Ballou.** 1996. Cell cycle regulation of p70 S6 kinase and p42/p44 mitogen-activated protein kinases in Swiss mouse 3T3 fibroblasts. J. Biol. Chem. **271:**963–971.
17. **Favata, M. F., K. Y. Horiuchi, E. J. Manos, A. J. Daulerio, D. A. Stradley, W. S. Feeser, D. E. Van Dyk, W. J. Pitts, R. A. Earl, F. Hobbs, R. A. Copeland, R. L. Magolda, P. A. Scherle, and J. M. Trzaskos.** 1998. Identification of a novel inhibitor of mitogen-activated protein kinase kinase. J. Biol. Chem. **273:**18623–18632.
18. **Gesbert, F., W. R. Sellers, S. Signoretti, M. Loda, and J. D. Griffin.** 2000. BCR/ABL regulates expression of the cyclin-dependent kinase inhibitor p27Kip1 through the phosphatidylinositol 3-kinase/AKT pathway. J. Biol. Chem. **275:**39223–39230.
19. **Gotoh, Y., E. Nishida, S. Matsuda, N. Shiina, H. Kosako, K. Shiokawa, T. Akiyama, K. Ohta, and H. Sakai.** 1991. In vitro effects on microtubule dynamics of purified *Xenopus* M phase-activated MAP kinase. Nature **349:**251–254.
20. **Gross, S. D., M. S. Schwab, F. E. Taieb, A. L. Lewellyn, Y. W. Qian, and J. L. Maller.** 2000. The critical role of the MAP kinase pathway in meiosis II in *Xenopus* oocytes is mediated by p90(Rsk). Curr. Biol. **10:**430–438.
21. **Guadagno, T. M., and J. E. Ferrell.** 1998. Requirement for MAPK activation

for normal mitotic progression in *Xenopus* egg extracts. Science **282:**1312–1315.
22. **Hitomi, M., and D. W. Stacey.** 1999. Cyclin D1 production in cycling cells depends on ras in a cell-cycle-specific manner. Curr. Biol. **9:**1075–1084.
23. **Hitomi, M., and D. W. Stacey.** 1999. Cellular ras and cyclin D1 are required during different cell cycle periods in cycling NIH 3T3 cells. Mol. Cell. Biol. **19:**4623–4632.
24. **Huang, C. Y., and J. E. Ferrell.** 1996. Dependence of Mos-induced Cdc2 activation on MAP kinase function in a cell-free system. EMBO J. **15:**2169–2173.
25. **Jesch, S. A., T. S. Lewis, N. G. Ahn, and A. D. Linstedt.** 2001. Mitotic phosphorylation of Golgi reassembly stacking protein 55 by MAP kinase ERK2. Mol. Biol. Cell **12:**1811–1817.
26. **Jones, S. M., and A. Kazlauskas.** 2001. Growth factor-dependent signaling and cell cycle progression. FEBS Lett. **490:**110–116.
27. **Jones, S. M., and A. Kazlauskas.** 2001. Growth-factor-dependent mitogenesis requires two distinct phases of signalling. Nat. Cell Biol. **3:**165–172.
28. **Kano, F., K. Takenaka, A. Yamamoto, K. Nagayama, E. Nishida, and M. Murata.** 2000. MEK and Cdc2 kinase are sequentially required for Golgi disassembly in MDCK cells by the mitotic *Xenopus* extracts. J. Cell Biol. **149:**357–368.
29. **Koranda, M., A. Schleiffer, L. Endler, and G. Ammerer.** 2000. Forkhead-like transcription factors recruit Ndd1 to the chromatin of G_2/M-specific promoters. Nature **406:**94–98.
30. **Kosako, H., Y. Gotoh, and E. Nishida.** 1994. Requirement for the MAP kinase kinase/MAP kinase cascade in *Xenopus* oocyte maturation. EMBO J. **13:**2131–2138.
31. **Kumar, R., D. M. Reynolds, A. Shevchenko, A. Shevchenko, S. D. Goldstone, and S. Dalton.** 2000. Forkhead transcription factors, Fkh1p and Fkh2p, collaborate with Mcm1p to control transcription required for M-phase. Curr. Biol. **10:**896–906.
32. **Laird, A. D., S. J. Taylor, M. Oberst, and D. Shalloway.** 1995. Raf-1 is activated during mitosis. J. Biol. Chem. **270:**26742–26745.
33. **Larijani, B., T. M.Barona, and D. L. Poccia.** 2001. Role for phosphatidylinositol in nuclear envelope formation. Biochem. J. **356:**495–501.
34. **Lewis, T. S., P. S. Shapiro, and N. G. Ahn.** 1998. Signal transduction through MAP kinase cascades. Adv. Cancer Res. **74:**49–139.
35. **Lukas, C., C. S. Sorensen, E. Kramer, E. Santoni-Rugiu, C. Lindeneg, J. M. Peters, J. Bartek, and J. Lukas.** 1999. Accumulation of cyclin B1 requires E2F and cyclin-A-dependent rearrangement of the anaphase-promoting complex. Nature **401:**815–818.
36. **Minshull, J., H. Sun, N. K. Tonks, and A. W. Murray.** 1994. A MAP kinase-dependent spindle assembly checkpoint in *Xenopus* egg extracts. Cell **79:**475–486.
37. **Murakami, M. S., T. D. Copeland, and G. F. Vande Woude.** 1999. Mos positively regulates Xe-Wee1 to lengthen the first mitotic cell cycle of *Xenopus*. Genes Dev. **13:**620–631.
38. **Nakajo, N., S. Yoshitome, J. Iwashita, M. Iida, K. Uto, S. Ueno, K. Okamoto, and N. Sagata.** 2000. Absence of Wee1 ensures the meiotic cell cycle in *Xenopus* oocytes. Genes Dev. **14:**328–338.
39. **Neighbors, B. W., R. C. Williams, Jr., and J. R. McIntosh.** 1988. Localization of kinesin in cultured cells. J. Cell Biol. **106:**1193–1204.
40. **Norman, B. H., C. Shih, J. E. Toth, J. E. Ray, J. A. Dodge, D. W. Johnson, P. G. Rutherford, R. M. Schultz, J. F. Worzalla, and C. J. Vlahos.** 1996. Studies on the mechanism of phosphatidylinositol 3-kinase inhibition by wortmannin and related analogs. J. Med. Chem. **39:**1106–1111.
41. **Pages, G., S. Guerin, D. Grall, F. Bonino, A. Smith, F. Anjuere, P. Auberger, and J. Pouyssegur.** 1999. Defective thymocyte maturation in p44 MAP kinase (Erk 1) knockout mice. Science **286:**1374–1377.
42. **Palmer, A., A. C. Gavin, and A. R. Nebreda.** 1998. A link between MAP kinase and p34(cdc2)/cyclin B during oocyte maturation: p90(rsk) phosphorylates and inactivates the p34(cdc2) inhibitory kinase Myt1. EMBO J. **17:**5037–5047.
43. **Pathan, N. I., C. L. Ashendel, R. L. Geahlen, and M. L. Harrison.** 1996. Activation of T cell Raf-1 at mitosis requires the protein-tyrosine kinase Lck. J. Biol. Chem. **271:**30315–30317.
44. **Pic, A., F. L. Lim, S. J. Ross, E. A. Veal, A. L. Johnson, M. R. Sultan, A. G. West, L. H. Johnston, A. D. Sharrocks, and B. A. Morgan.** 2000. The forkhead protein Fkh2 is a component of the yeast cell cycle transcription factor SFF. EMBO J. **19:**3750–3761.
45. **Roche, S., S. Fumagalli, and S. A. Courtneidge.** 1995. Requirement for Src family protein tyrosine kinases in G_2 for fibroblast cell division. Science **269:**1567–1569.
46. **Sagata, N.** 1997. What does Mos do in oocytes and somatic cells? Bioessays **19:**13–21.
47. **Sebolt-Leopold, J. S., D. T. Dudley, R. Herrera, K. Van Becelaere, A. Wiland, R. C. Gowan, H. Tecle, S. D. Barrett, A. Bridges, S. Przybranowski, W. R. Leopold, and A. R. Saltiel.** 1999. Blockade of the MAP kinase pathway suppresses growth of colon tumors in vivo. Nat. Med. **5:**810–816.
48. **Shapiro, P. S., E. Vaisberg, A. J. Hunt, N. S. Tolwinski, A. M. Whalen, J. R. McIntosh, and N. G. Ahn.** 1998. Activation of the MKK/ERK pathway during somatic cell mitosis: direct interactions of active ERK with kinetochores and regulation of the mitotic 3F3/2 phosphoantigen. J. Cell Biol. **142:**1533–1545.
49. **Shapiro, P. S., and N. G. Ahn.** 1998. Feedback regulation of Raf-1 and mitogen-activated protein kinase (MAP) kinase kinases 1 and 2 by MAP kinase phosphatase-1 (MKP-1). J. Biol. Chem. **273:**1788–1793.
50. **Shtivelman, E., J. Sussman, and D. Stokoe.** 2002. A Role for PI 3-kinase and PKB activity in the G_2/M phase of the cell cycle. Curr. Biol. **12:**919–924.
51. **Sif, S., P. T. Stukenberg, M. W. Kirschner, and R. E. Kingston.** 1998. Mitotic inactivation of a human SWI/SNF chromatin remodeling complex. Genes Dev. **12:**2842–2851.
52. **Takenaka, K., Y. Gotoh, and E. Nishida.** 1997. MAP kinase is required for the spindle assembly checkpoint but is dispensable for the normal M phase entry and exit in *Xenopus* egg cell cycle extracts. J. Cell Biol. **136:**1091–1097.
53. **Tamemoto, H., T. Kadowaki, K. Tobe, K. Ueki, T. Izumi, Y. Chatani, M. Kohno, M. Kasuga, Y. Yazaki, and Y. Akanuma.** 1992. Biphasic activation of two mitogen-activated protein kinases during the cell cycle in mammalian cells. J. Biol. Chem. **267:**20293–20297.
54. **Vlahos, C. J., W. F. Matter, K. Y. Hui, and R. F. Brown.** 1994. A specific inhibitor of phosphatidylinositol 3-kinase, 2-(4-morpholinyl)-8-phenyl-4H-1-benzopyran-4-one (LY294002). J. Biol. Chem. **269:**5241–5248.
55. **Walter, S. A., S. N. Guadagno, and J. E. Ferrell.** 2000. Activation of Wee1 by p42 MAPK in vitro and in cycling *Xenopus* egg extracts. Mol. Biol. Cell **11:**887–896.
56. **Walter, S. A., T. M. Guadagno, and J. E. Ferrell.** 1997. Induction of a G_2-phase arrest in *Xenopus* egg extracts by activation of p42 mitogen-activated protein kinase. Mol. Biol. Cell **8:**2157–2169.
57. **Wang, X. M., Y. Zhai, and J. E. Ferrell.** 1997. A role for mitogen-activated protein kinase in the spindle assembly checkpoint in XTC cells. J. Cell Biol. **137:**433–443.
58. **Wood, K. W., R. Sakowicz, L. S. Goldstein, and D. W. Cleveland.** 1997. CENP-E is a plus end-directed kinetochore motor required for metaphase chromosome alignment. Cell **91:**357–366.
59. **Wright, J. H., E. Munar, D. R. Jameson, P. R. Andreassen, R. L. Margolis, R. Seger, and E. G. Krebs.** 1999. Mitogen-activated protein kinase kinase activity is required for the G_2/M transition of the cell cycle in mammalian fibroblasts. Proc. Natl. Acad. Sci. USA **96:**11335–11340.
60. **Zecevic, M., A. D. Catling, S. T. Eblen, L. Renzi, J. C. Hittle, T. J. Yen, G. J. Gorbsky, and M. J. Weber.** 1998. Active MAP kinase in mitosis: localization at kinetochores and association with the motor protein CENP-E. J. Cell Biol. **142:**1547–1558.
61. **Zheng, X. M., and D. Shalloway.** 2001. Two mechanisms activate PTPalpha during mitosis. EMBO J. **20:**6037–6049.
62. **Zheng, X. M., R. J. Resnick, and D. Shalloway.** 2002. Mitotic activation of protein-tyrosine phosphatase alpha and regulation of its Src-mediated transforming activity by its sites of protein kinase C phosphorylation. J. Biol. Chem. **277:**21922–21929.